

000 BEYOND MARKOVIAN DRIFTS: ACTION-BIASED GE- 001 OMETRIC WALKS WITH MEMORY FOR PERSONALIZED 002 SUMMARIZATION

006 **Anonymous authors**

007 Paper under double-blind review

011 ABSTRACT

013 Personalized document summarization helps readers focus on the “content-of-
 014 *interest*”, a *subjective* and *time-variant* quantity. Recent news recommendation
 015 and summarization models often assume that preferences follow a *memoryless*
 016 or *short-memory random walk* on interaction graphs, i.e., a Markovian diffusion
 017 seeded at the latest interaction or compressed into a short hidden state or prompt.
 018 We ask whether such a hypothesis also holds for personalized summarization.
 019 To this end, we propose **Walk2Pers**, a lightweight encoder-decoder framework
 020 that extends the walk view with *action-conditioned geometric steps*, decomposed
 021 into a (i) a *magnitude* controlling shift strength, and (ii) an *orientation* capturing
 022 continuity vs. novelty. The process is mediated by dual memory lanes that rein-
 023 force consistent interests while suppressing disinterest, and is augmented with a
 024 drift term for summary requests. We show theoretically that such structured walks
 025 approximate first-order action-conditioned kernels, and empirically validate the
 026 hypothesis on three benchmark datasets – PENS, OpenAI-Reddit, and Personal-
 027 Sum. Using PerSEval, a personalization metric with strong human correlation,
 028 Walk2Pers outperforms specialized personalized summarizers by an average of
 029 $0.41 \uparrow$, and strong LLM baselines (DeepSeek-R1-14B, LLaMA-2-13B, Mistral-
 030 7B, Zephyr-7B) by $0.22 \uparrow$. Our analyses further confirm cross-domain robustness
 031 ($0.19 \uparrow$ over the best LLM) and stability on long histories. Together, these results
 032 support viewing personalized summarization as an *action-biased geometric walk*
 033 with *memory*, offering both interpretability and efficiency.

034 1 INTRODUCTION

036 With the problem of information overload, personalized summarization has become essential for
 037 tailoring updates to a reader’s individual interests, especially in multi-aspect documents covering
 038 diverse topics (Dasgupta et al., 2024). Existing approaches typically rely on *static* persona attributes
 039 (Dou et al., 2021; He et al., 2022; Li et al., 2023). Yet, datasets capturing user reading behav-
 040 iors, such as MS/CAS PENS (Ao et al., 2021), reveal that user preferences evolve over time and
 041 shift across fine-grained subtopics. This creates difficulties even for state-of-the-art (SOTA) Large
 042 Language Models (LLMs), which show degraded performance when long user-interaction histories
 043 are embedded in prompts for in-context personalized summarization (Liu et al., 2024; Patel et al.,
 044 2024). This suggests that both existing personalized summarizers and LLMs struggle to capture
 045 subtle, action-specific user interactions within user logs.

046 A natural follow-up question is *how do user preferences predictably evolve over time?* In most
 047 recommendation and personalized summarization systems, user preference evolution has been mod-
 048 eled using simple Markovian assumptions, the most basic case being *pure Random Walk*, where
 049 each new preference state is treated as an isotropic perturbation of the previous one, without any
 050 action semantics conditioning. A stronger variant is the *Action-conditioned Random Walk*, which
 051 biases each step by the most recent action type, while still remaining memoryless. More recently,
 052 graph-based *Random Walk with Restart* (RWR) methods, including Personalized PageRank and its
 053 extensions, have been widely applied in news recommendation, where user interests are modeled
 as a diffusion process seeded at the last interaction. Notably, S-Walk (Qiu et al., 2022) restructures
 the transition kernel to improve session-level modeling, and D-RDW (Zhang et al., 2025) diversifies

restart paths to mitigate popularity bias. Although these models remain competitive as *lightweight graph baselines*, extensive benchmarking under the same evaluation regimes (e.g., MIND, Adressa) has shown them to be outperformed by neural encoders such as NAML (Wu et al., 2019a), NRMS (Wu et al., 2019b), and EBNR (Okura et al., 2017), which aggregate user click histories via CNNs, Transformers, or GRUs. However, these models reduce long histories into compressed embeddings, providing only shallow memory. Similarly, preference-prompted mid-sized LLM summarizers can condition on past interactions, although their windowed prompts impose a hard memory cap, with no persistent reinforcement or suppression. Collectively, graph-based diffusion, short-memory neural encoders, and prompt-based LLMs fall under the *Markovian Drift Hypothesis (MDH)* – *each new state depends primarily on the most recent interaction, overriding long-horizon action dynamics*.

In this paper, we test how well MDH holds for personalized summarization. As an alternative extension to MDH, we propose the Structured Walk Hypothesis (SWH). SWH decomposes the preference state update due to each user interaction (*click*, *skip*, *summarize*) into (i) a *magnitude*, controlling the strength of the action-specific nudge, and (ii) an *orientation*, determining whether the evolution follows the existing trajectory (continuity) or departs into a new direction (novelty). In this way, SWH is an *action-conditioned geometric walk*. To go beyond MDH, SWH incorporates dual memory lanes that reinforce consistent interests while suppressing disinterest (for a comparative table of SOTA MDH models see Table 10). We propose **Walk2Pers**, a personalized summarization model, as a concrete realization of SWH. To test the adequacy of MDH, we pose three research questions. **RQ1:** *Is MDH sufficient for modeling preference evolution in summarization?* **RQ2:** *Do dual memory lanes and action-conditioned geometric steps with magnitude–orientation decomposition, provide systematic and complementary gains over MDH variants?* **RQ3:** *How does Walk2Pers, as an instantiation of SWH, compare against short-memory neural encoder augmented personalized summarizers, prompt-personalized LLMs, and oracle summarizers?*

For **RQ1** and **RQ2**, we benchmark MDH-based neural encoder models, along with our own simple action-conditioned Short-Memory Drift (SMD) and an action-category sensitive Action-Gated drift (AGD), on the next user behavior prediction task. We show that these MDH baselines do not sustain asymmetric reinforcement / suppression or disentangle continuity from novelty. In contrast, structured walks with dual memory and geometric decomposition achieve systematic gains, with Walk2Pers outperforming the best AGD model by **0.07/0.12/0.18**↑ w.r.t AUC/MRR/nDCG@5/10 metrics. For **RQ3**, we assess downstream personalized summarization. On the PENS dataset, Walk2Pers surpasses specialized summarizers (PENS-NAML, NRMS, EBNR, GTP, SP) by an average of **0.42/0.36/0.43**↑ across personalization metrics (PSE-JSD/SU4/METEOR). It also outperforms four mid-sized LLMs (Zephyr-7B, LLaMA2-13B, Mistral-7B, DeepSeek-R1-14B) under 2-shot+history prompting (the best configuration), with DeepSeek-R1 lagging by **0.20/0.29/0.35**. Together, these results demonstrate that while MDH models can be competitive in recommendation-style ranking, SWH with explicit magnitude-orientation decomposition, dual memories, and drift, faithfully captures evolving user preferences for personalized summarization.

2 RELATED WORK

Personalized Summarization Evaluation. Personalized summarization has been increasingly recognized as essential for tailoring updates to a reader’s interests, especially when documents cover multiple aspects. Existing evaluations of summarization quality (e.g., ROUGE, METEOR, BLEU) do not explicitly account for personalization. Recent work (Vansh et al., 2023; Dasgupta et al., 2024) has emphasized the need for personalization-aware metrics. EGISES proposed a framework for evaluating semantic shift under personalization, while Dasgupta et al. (2024) introduced **PerSE-val**, which we adopt in this paper as it correlates strongly with human judgment.

Datasets for personalized summarization. To study evolving user preferences, we require datasets with (i) temporal orders of user interactions, (ii) user-specific expected summaries for shared contents, and (iii) diverse, shifting topics and subtopics. In this direction, the MS/CAS **PENS** dataset (Ao et al., 2021) contains click/skip logs with multi-aspect articles and user-target summaries (per trajectory: 13.6 topics; 52.83 sub-topics, with topic change rate of 0.77). It has become a benchmark for testing personalization-aware models (Ao et al., 2021; Song et al., 2023; Lian et al., 2025). **PersonalSum** (Zhang et al., 2024), The Norwegian dataset derived from Adressa, augments news interaction logs with personalized gold summaries. It highlights preference drift and is suitable for

108 multilingual evaluation. **OpenAI-Reddit** (Völske et al., 2017) provides long-range user interaction
 109 traces (posts and comments) with subjective summaries. This non-news multi-domain dataset
 110 stresses long-horizon dependencies and temporal drift, and is used for cross-domain generalizability
 111 test. Dataset details are in Appendix C.

112 **Personalized Summarization Models.** Most existing personalized summarizers rely on *static* user
 113 personas, as in GSUM, CTRLSum, TMWIN, and Tri-Agent (Dou et al., 2021; He et al., 2022;
 114 Kirstein et al., 2024; Xiao et al., 2024). Dynamic extensions such as PENS (Ao et al., 2021) in-
 115 incorporate external news-recommendation encoders like NRMS Wu et al. (2019b), NAML Wu et al.
 116 (2019a), and EBNR Okura et al. (2017), while GTP (Song et al., 2023) leverages latent editing
 117 controls and SCAPE (Lian et al., 2025) blends content with stylistic features. However, these ap-
 118 proaches remain within the scope of the MDH. The few-shot LLM personalization (Patel et al.,
 119 2024) achieves competitive performance against such models, but is ultimately stalled by prompt
 120 length and memory constraints. In contrast, our work explores SWH, where preference evolution is
 121 modeled as a memory-aware, action-conditioned geometric walk. `Walk2Pers` serves as one concrete
 122 instantiation capturing evolving user histories beyond the limits of MDH-style summarizers.

124 3 METHODOLOGY: USER PREFERENCE EVOLUTION REPRESENTATION

126 3.1 PREFERENCE DATA AS USER-INTERACTION GRAPH (UIG)

128 We represent user histories as a **User-Interaction Graph** (UIG), a directed acyclic graph $G =$
 129 $\langle N, E \rangle$ where the node set N consists of three disjoint types: (i) **u-nodes** $u^{(t_0)}$ denoting a user at
 130 initial timestep t_0 , (ii) **d-nodes** $d^{(t_i)}$ representing documents interacted at timestep t_i , and (iii) **s-
 131 nodes** $s_u^{(t_j)}$ representing user-specific summaries requested or generated at time t_j for a document
 132 viewed at t_{j-1} . The edge set E encodes user actions: $a_d^{(t_i)} \in \{\text{click, skip, summarize}\}$
 133 on documents, and $a_s^{(t_j)}$ as the follow-up `summGen` action connecting a document $d^{(t_{j-1})}$ to its
 134 summary $s_u^{(t_j)}$. A user trajectory τ_u is then a time-ordered sequence of such interactions, beginning
 135 at $u^{(t_0)}$. Each trajectory can be decomposed into *behavior duplets* $b_u^{(t_i)} = \langle a^{(t_i)}, tl^{(t_i)} \rangle$, pairing an
 136 action with its tail node $tl^{(t_i)}$. The UIG \mathcal{T} is a pool of trajectories, used as $\mathcal{T}_{\text{train}}$ for training and $\mathcal{T}_{\text{test}}$
 137 for evaluation. For UIG construction, see Appendix C.4; Figure 4.

139 While UIG captures rich temporal detail, directly modeling its raw structure quickly becomes com-
 140 putationally expensive and noisy over long horizons. This is particularly challenging in personalized
 141 summarization, where fine-grained shifts in preference must be retained without overwhelming the
 142 model. Recent work in sequential recommendation suggests that *hierarchical abstractions* improve
 143 long-horizon accuracy by condensing low-level interactions into higher-order behavioral units (Cho
 144 & Hyun, 2023; Ou et al., 2025; Zhu et al., 2023; Pan & Wang, 2021; Zhang et al., 2020). Motivated
 145 by this, we adopt a bi-level hierarchy – the **u-layer** records raw interactions: user nodes $u^{(t_0)}$, docu-
 146 ment nodes $d^{(t)}$, and summary nodes $s^{(t)}$, connected by action edges $a^{(t)}$, and the **b-layer** abstracts
 147 these into *behavior duplets* $b_{u_j}^{(t)} = \langle a^{(t)}, tl^{(t)} \rangle$, represented as **b-nodes**. Sequential dependencies
 148 are captured by `nextBehavior` edges. This abstraction provides a compact yet expressive substrate
 149 for modeling preference evolution. Having established the representational basis, we now ask a
 150 fundamental question: *how do preferences evolve along b-layer trajectories?*

152 3.2 MODELING USER PREFERENCE EVOLUTION

153 We model preference evolution on the b-layer. Each visited b-node $b_u^{(t)}$ is associated with a latent
 154 preference embedding $e_{b,u}^{(t)} \in \mathbb{R}^d$ summarizing user u 's state after timestep t . We first state the
 155 prevailing *Markovian Drift* assumption, then contrast it with our *Structured Walk Hypothesis*.

157 3.2.1 MARKOVIAN DRIFT HYPOTHESIS (MDH)

159 Under MDH, the next state depends only on the immediately preceding state (or a short compressed
 160 representation), while longer histories are discounted or collapsed into a recency prior q :

$$161 e_{b,u}^{(t+1)} = f(e_{b,u}^{(t)}, a^{(t)}, q) + \epsilon^{(t)}, \quad \epsilon^{(t)} \sim \mathcal{N}(0, \Sigma(a^{(t)})). \quad (1)$$

162

163 Table 1: **SWH (vs. MDH)**: (i) explicit **trajectory modeling** across b -nodes, (ii) dual **memory lanes**
164 (h^+, h^-) for reinforcement and suppression, and (iii) **action-aware updates** per $a^{(t)}$.

Aspect	Markovian Drift Hypothesis	Structured Walk Hypothesis
History usage	Collapsed into last state or seed q	Explicit trajectory across b -nodes
Memory	None or short-lived (hidden states, attention)	Dual memory lanes (h^+, h^-) for reinforcement/suppression
Action conditioning	Minimal (recency, weak prompt)	Explicit action-aware updates per $a^{(t)}$
Step dynamics	<i>Magnitude</i> : implicit (via GRU/attention weights/prompt tokens)	<i>Magnitude</i> : $\text{mag}(a^{(t)})$
Long-term preferences	<i>Orientation</i> : not modeled explicitly	<i>Orientation</i> : $\theta(a^{(t)})$
Interpretability	Forgotten beyond 1 step	Persist through memory-conditioned updates
	Opaque embeddings/hidden states	Geometric (continuity vs. novelty) and stochastic (controlled walk)

170

171

172 Here $\Sigma(a^{(t)}) \in \mathbb{R}^{d \times d}$ controls how stochastic drift spreads across embedding dimensions. The
173 action-conditioning lets skips be noisier than focused clicks. A pure Random Walk (PRW) is:
174 $f(e_{b,u}^{(t)}, a^{(t)}, q) = e_{b,u}^{(t)}$. Short-memory neural encoders (NAML, NRMS, EBNR) and prompt-
175 personalized LLMs also fit this umbrella by compressing history into short-term aggregates.

176

177 3.2.2 STRUCTURED WALK HYPOTHESIS (SWH)
178

179 Evidence from PENS (Ao et al., 2021), PersonalSum (Zhang et al., 2024), and OpenAI-Reddit
180 (Völkske et al., 2017) indicates long-horizon dependencies: clicks reinforce, skips suppress, and
181 summary requests induce systematic drifts. We posit the **SWH**: *preference evolution is a structured,*
182 *action-conditioned geometric walk with memory*:

$$183 \quad e_{b,u}^{(t+1)} = e_{b,u}^{(t)} + \Phi(a^{(t)}, \text{trajectory-context}) + \Psi(h_t^+, h_t^-) + \Delta(a^{(t)}), \quad (2)$$

185

186 where $\Phi(\cdot)$ decomposes trajectory-context into a *momentum* direction $u^{(t)}$ (continuity) and an
187 *orthogonal novelty* direction $o^{(t)}$, $\Psi(\cdot)$ aggregates asymmetric reinforcement/suppression via
188 (h_t^+, h_t^-), and $\Delta(\cdot)$ captures special action drifts (e.g., `summGen`). This decomposition is inspired
189 by advances in trajectory-based dynamic embeddings (e.g., JODIE (Kumar et al., 2019a)) and angle-
190 based relational models (e.g., RotateE, ChronoR (Sun et al., 2019; Anshelevich et al., 2021)), but
191 adapted to the summarization setting with explicit action bias and memory. To illustrate, frequent
192 climate-policy clicks keep movement near $u^{(t)}$ and accumulate in h_t^+ ; repeated skips of celebrity
193 content load h_t^- and downweight entertainment; issuing `summGen` after dense reports triggers $\Delta(\cdot)$,
194 nudging toward concise representations. This view generalizes random walks into a controlled dif-
195 fusion governed by state, action, and memory traces (Kumar et al., 2019b; Balcer & Lipinski, 2025).

196

197 **SWH Model Family.** Refining Eq. equation 2, we obtain a generic *structured walk* family:

$$198 \quad e_{b,u}^{(t+1)} = e_{b,u}^{(t)} + \underbrace{\text{mag}(a^{(t)}) (\cos \theta(a^{(t)}) u^{(t)} + \sin \theta(a^{(t)}) o^{(t)})}_{\Phi: \text{geometric step: continuity vs. novelty}} \\ 199 \quad + \underbrace{\Psi(h_t^+, h_t^-)}_{\Psi: \text{dual memory: reinforcement vs. suppression}} + \underbrace{\delta \cdot \mathbb{I}[a^{(t)} = \text{summGen}]}_{\Delta: \text{summary-specific drift}}. \quad (3)$$

200

201

202

203

204 Here $\text{mag}(a^{(t)})$ scales the step (single click = small shift; repeated clicks = larger shift). The angle
205 $\theta(a^{(t)})$ steers between $u^{(t)}$ and $o^{(t)}$: small θ (so $\cos \theta \approx 1, \sin \theta \approx 0$) favors continuity; larger θ in-
206 creases novelty. $\Psi(h_t^+, h_t^-)$ persists asymmetric signals from past actions, and the drift δ (active for
207 `summGen`) captures shifts due to specific interest signal. Different models may parameterize mag ,
208 θ , and Ψ differently, but all share this decomposition. In the next section, we present `Walk2Pers`
209 as one concrete instantiation of this family. Theoretical relationship to the MDH is in Appendix D.

210

211 3.3 **WALK2PERS** MODEL AS SWH INSTANTIATION
212213 3.3.1 WALK2PERS ENCODER: HISTORY ENCODING WITH STRUCTURED WALKS
214

215 We instantiate SWH (Eq. 3) in `Walk2Pers` by encoding user trajectories as action-aware b-cells,
216 augmented with dual memories for persistence and geometric steps for continuity–novelty tradeoff.

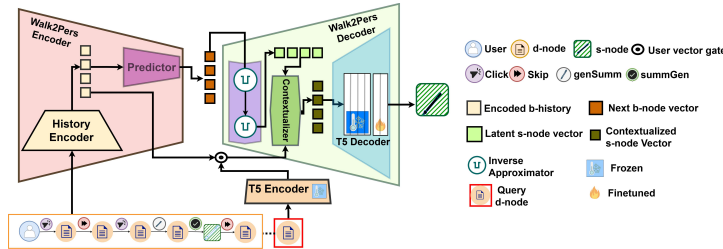


Figure 1: **Walk2Pers**: Novel instantiation of SWH – b-node embedding is formed from the u-layer and fed into the **SWH-Encoder**; **Predictor** estimates the next b-node, the embedding of which is fed into the **Inverse Approximator**, which extracts the latent summary (s-node); **Contextualizer** computes cross-attention of latent s-node, user history, with query document; **T5-decoder** finetuned (top-layers only) to generate personalized summary. b-node embedding details in Figure 2.

Action-biased B-cell composition. Each d-node and s-node is initialized with a T5-base encoder (Raffel et al., 2020), while each action at timestep t_i is represented as a 4-d one-hot vector (*click*, *skip*, *summarize*, *summGen*). A b-cell fuses the action with its tail-node content: $c_{tl}^{(t_i)} = \tanh(f^{(a,t_i)}) \odot e_{tl}^{(t_i)}$; $e_{b,u}^{(t_i)} = \tanh(W_b \cdot c_{tl}^{(t_i)})$. where $f^{(a,t)}$ is an *action-conditioned gate*. We borrow the AGD(\cdot) function of the baseline Action-Gated Drift model (AGD) (Section 4.2; Appendix E.1), which generates action-specific $f^{(a,t)}$ for action type (*click*, *skip*, *summarize*, *summGen*). Here, *click* strengthens the fused representation, *skip* weakens it, and *summGen* anchors it to a summary node.

Dual memories and drift (Realization of Ψ and Δ). To capture long-term asymmetries, Walk2Pers models history as a linear combination of dual memory lanes: $\mathbf{h}^{(t)} = \omega^{(t)} \mathbf{h}^{(+,t)} + (1 - \omega^{(t)}) \mathbf{h}^{(-,t)}$ (ω is learnable scalar), where $\mathbf{h}^{(+)}$ accumulates reinforcement signals (clicks), and $\mathbf{h}^{(-)}$ accumulates suppression signals (skips) as follows:

$$\mathbf{h}^{(+,t_i)} = \mathbf{h}^{(+,t_{i-1})} + m^{(t_i)} \odot \mathbf{c}_{tl}^{(t_i)}; \mathbf{h}^{(-,t_i)} = \mathbf{h}^{(-,t_{i-1})} \odot (1 - m^{(t_i)}) + \mathbf{c}_{tl}^{(t_i)}. \quad (4)$$

In case where the action is *summGen*, triggering a drift vector $\Delta^{(t)}$, $\mathbf{h}^{(+,t_i)} = \mathbf{h}^{(+,t_{i-1})} + m^{(t_i)} \odot \Delta^{(t)}$, where $\Delta^{(t)} = (\mathbf{I} - \mathbf{e}_{tl}^{(t-1)}) \cdot \mathbf{e}_{tl}^{(t)}$, and $m^{(t_i)} = \text{SoftMax}(\mathbf{W}_h \cdot \mathbf{h}^{(t_{i-1})} + \mathbf{W}_c \cdot \mathbf{c}_{tl}^{(t_i)})$. Δ nudges the preference state toward condensed representations since *summarize*–*summGen* is a stronger positive signal. The corresponding action-gate is then applied as: $f^{(a,t_i)} = \text{AGD}(\mathbf{e}_a, t_i) \odot \mathbf{h}^{(t)}$ (see Appendix E.1). The b-node embedding is computed as $e_{b,u}^{(t_i)} = \tanh(W_b \cdot (\tanh(f^{(a,t_i)}) \odot e_{tl}^{(t_i)}))$.

Geometric step decomposition. Finally, Walk2Pers models preference evolution as a directed, structured geometric step, balancing persistence with novelty $\Phi(\cdot)$:

$$\mathbf{e}^{c^{(t)}} = e_{b,u}^{(t)} + \text{mag}^{(t)} \left(\cos \theta^{(t)} \cdot u^{(t-1)} + \sin \theta^{(t)} \cdot o^{(t)} \right), \quad (5)$$

where $u^{(t-1)}$ is the momentum axis (continuity), $o^{(t)}$ its orthogonal novelty axis, $\text{mag}^{(t)}$ the step size, and $\theta^{(t)}$ the rotation angle interpolating between persistence ($\theta \approx 0$) and novelty (θ large). This realizes the Φ term in & Eq. 3 (Implementation & theoretical equivalence: Appendices G G.2).

Training. The encoder is supervised via two complementary objectives. First, the *next-node prediction head* maps the final contextualized embedding to the predicted query b-node: $\mathbf{e}_{b_q,u}^{(t+1)} = \mathbf{W}_{\text{next}} \cdot \mathbf{e}_{b,u}^{(t)} + b_{\text{next}}$. Second, a *position classifier* enforces alignment between the contextualized trajectory and its constituent steps: $\hat{\mathbf{p}}_b^{(t)} = \text{SoftMax}(W_{\text{pos}} \cdot \mathbf{e}_{b,u}^{(t)})$. The joint objective combines these two signals: $\mathcal{L}_{\text{align}} = -\frac{1}{l} \sum_{i=1}^l \log \hat{p}_b^{(t_i)}$; $\mathcal{L}_{\text{next}} = -\log \hat{p}_b^{(t)}$; $\mathcal{L}_{\text{enc}} = \alpha \mathcal{L}_{\text{align}} + (1 - \alpha) \mathcal{L}_{\text{next}}$; $\alpha = 0.6$ so as to avoid cumulative cascading of $\mathcal{L}_{\text{align}}$ on $\mathcal{L}_{\text{next}}$. The alignment term ensures that each intermediate b-node in the trajectory is recoverable from the contextualized embedding, regularizing the walk so it respects positional consistency across steps. The next-node prediction term directly

270 trains the encoder to forecast the upcoming behavior node, making the walk predictive rather than
 271 descriptive. Together, these losses encourage Φ (geometric step), Ψ (dual memories), and Δ (drift)
 272 to cooperate in producing embeddings that are both history-faithful and forward-looking.
 273

274 **3.3.2 DECODER: CONTEXTUALIZING USER INTENT FOR SUMMARIZATION**
 275

276 While the encoder (Sec. 3.3.1) is the core instantiation of the Structured Walk Hypothesis, we at-
 277 tach the same backbone decoder of the encoder-decoder model used to generate seed embeddings,
 278 T5-base, that consumes the contextualized query embedding $e_{d_{q,u}}^c$ and generates the personalized
 279 summary. Training optimizes a combined objective: $\mathcal{L}_{\text{dec}} = \text{Average}(\mathcal{L}_{\text{gen}}, \mathcal{L}_{\text{enc}})$, where \mathcal{L}_{gen} is
 280 cross-entropy under teacher forcing and \mathcal{L}_{enc} is the structured-walk encoder loss from Sec. 3.3.1.
 281 This ensures that the encoder faithfully models user trajectories while the decoder exploits those
 282 states to produce preference-aware summaries. We evaluate two decoder variants: **T5-CA (Con-
 283 texualized Attention)** and **T5-UCA (User-aware CA)**. The T5-CA-Decoder contextualizes the query
 284 document embedding e_{d_q} with the latent summary intention vector (s-node) via cross-attention.
 285 This injects *summary intent* but leaves the document representation agnostic of the user’s history.
 286 T5-UCA-Decoder builds on that by gating the query document embedding with the user’s trajec-
 287 tory state $e_{q,b_{u_j}}^{(t_l)}$. The gating suppresses aspects aligned with h^- (e.g., topics repeatedly skipped)
 288 and amplifies aspects aligned with h^+ (reinforced interests), producing a user-aware document vec-
 289 tor. This ensures that the same document is viewed through Alice’s preference lens differently than
 290 through Bob’s. The gated representation is then contextualized with the latent summary intent, as in
 291 CA. While CA adapts summaries to “*what this document is generally about given the latent sum-
 292 mary signal*”, UCA further adapts to “*what this document means for this user given their interaction
 293 history*.” As shown in Sec. 5.2, UCA yields stronger personalization, while CA serves as a weaker
 294 control. Full derivations of latent s-node extraction and gating functions are in Appendix G.3.
 295

296 **4 EVALUATION**
 297

298 We design the experiments to address the following research questions (RQ): **RQ1:** Is MDH suffi-
 299 cient for modeling preference evolution in summarization? **RQ2:** Do the necessary components of
 300 the SWH, i.e., dual memory lanes + summary-specific drift & action-conditioned geometric steps
 301 with magnitude–orientation decomposition, yield systematic gains over MDH variants? **RQ3:** How
 302 does `Walk2Pers`, as an instantiation of SWH, compare against specialized personalized summa-
 303 rizers, prompt-personalized LLMs, and oracle summarizers?
 304

305 **4.1 EXPERIMENT SETUP**
 306

307 **Training (& Test) Datasets.** We evaluate across three corpora capturing diverse personalization
 308 signals: (i) **PENS** (Ao et al., 2021), a large-scale news summarization dataset with user clicks/skips;
 309 (ii) **PersonalSum (EN)** (Zhang et al., 2024), a manually curated dataset translated to English with
 310 explicit summary requests; (iii) **OpenAI-Reddit** (Völske et al., 2017), where summaries are user-
 311 rated and span diverse domains. We construct UIGs for each dataset $\mathcal{T}_{\text{train}}$ and slice trajectories be-
 312 fore every $(d-s)$ pair, yielding history $\tau_h^{u_j}$, query document d_q , and target summary s_{q,u_j}^* . For PENS
 313 ($\mathcal{T}_{\text{train}}^{\text{PENS-D}}$), we sample 55K training trajectories (avg. 134 d -nodes, 5 s -nodes per trajectory). For
 314 OpenAI-Reddit ($\mathcal{T}_{\text{train}}^{\text{OAI}}$), 18K training trajectories (avg. 39 d -nodes, 10 s -nodes per trajectory). For
 315 PersonalSum-EN ($\mathcal{T}_{\text{train}}^{\text{PS-EN}}$) (translated into English using M2M-100 (Fan et al., 2020)), 700 trajec-
 316 tories (highly curated, long-horizon). The corresponding Test sets ($\mathcal{T}_{\text{test}}$) reflect the same structure,
 317 with additional random skips injected (50–70 per user in PENS) to stress-test suppression memory¹.
 318

319 **Training Setup.** `Walk2Pers` is trained end-to-end with the joint encoder–decoder objective \mathcal{L}_{dec}
 320 for 6 epochs. Then the encoder is frozen while the decoder (including the last 6 layers of the T5
 321 decoder) is further finetuned for 18 epochs. This ensures encoder quality is the primary driver of
 322 downstream summarization gains. Training details are in Appendix H.2 and Table 13.
 323

¹For detailed stress test results see Appendix I.2 and I.3.

324
325

4.2 BASELINES

326

A. Encoder Baselines We benchmark `Walk2Pers` for **RQ-1 & 2** against five MDH models:

327

I. Short-Memory Drift (SMD). This minimal baseline captures the pure MDH stance: each new b-node embedding is computed only from the immediate past state and the current action embedding. No reinforcement, suppression, or geometric structure is retained. User preference evolution reduces to a one-step drift, overwriting longer histories. Details in Appendix E.1.

331

II. Action-Gated Drift (AGD). This stronger MDH variant replaces the update rule of SMD with action-specific gates. Different parameterizations are applied for `click`, `skip`, `genSumm`, and `summGen`, allowing the model to qualitatively differentiate between actions. However, the updates remain short-memory: past interactions vanish quickly, and no persistent reinforcement or suppression is maintained. Details in Appendix E.1.

336

III. Short-Memory Neural-Encoders. We also include **NAML** (Wu et al., 2019a), **NRMS** (Wu et al., 2019b), and **EBNR** (Okura et al., 2017), widely used in personalized recommendation and summarization pipelines (e.g., PENS). These models differ in mechanism. NAML employs additive self-attention over multi-view document features, NRMS uses multi-head self-attention, and EBNR leverages a GRU over clicked entities. However, all collapse long histories into compressed short-memory embeddings, consistent with MDH.

342

These baselines constitute strong MDH realizations for the **next-b-node prediction task**. The candidate set contains 151 b-nodes (including the target). We report average AUC, MRR, and nDCG@5/10 over the PENS test set (metric definitions in Appendix B), with full baseline formalizations in Appendix E.1. These metrics directly measure a model’s ability to predict real user behavior because each ground-truth b-node corresponds to an actual user action (`click`, `skip`, `summarize`) and, for $\langle \text{sumGen}, \text{s-node} \rangle$ pairs, to a **human-written summary**. Hence, RQ1/2 evaluate *behavioral faithfulness*.

349

B. Personalized Summarizers To validate the efficacy of `Walk2Pers` in terms of the downstream personalized summarization task, we also compare against SOTA personalized summarizers.

352

I. Neural-Encoder Augmented Summarizers. For **RQ-3**, we compare against three SOTA personalized summarizers: PENS (Ao et al., 2021), GTP (Song et al., 2023), and Signature-Phrase (Cai et al., 2023). PENS pairs a pointer generator with external user encoders; GTP integrates the TrRMIo encoder internally. Within PENS, we use NAML (Wu et al., 2019a) (T-1), EBNR (Okura et al., 2017) (T-1), and NRMS (Wu et al., 2019b) (T-2), with injection (T-x) details in Appendix E.2.1. TrRMIo is an integrated full-sequence Transformer, while Signature-Phrase models user-specific keyphrases. All baselines are finetuned on $\mathcal{T}_{\text{train}}^P$ under the same regime as `Walk2Pers`.

358

II. LLMs-as-Summarizers. To extend **RQ-3**, we evaluate six **frozen** instruction-tuned LLMs—Gemini-2.5-Flash, Qwen3-235B (Team, 2025), Mistral-7B-Instruct (Jiang et al., 2023), DeepSeek-R1-14B (DeepSeek-AI et al., 2025), LLaMA-2-13B-Chat-HF (Touvron et al., 2023), and Zephyr-7B (Tunstall et al., 2023). Gemini and Qwen are included for their SOTA LongBench performance. We use the best 0-shot and 2-shot prompting recipes from Patel et al. (2024) and apply prompt-chaining for DeepSeek-R1-14B and Mistral-7B-Instruct. Prompt formats are in Appendix J.

360

III. Non-Personalized Summarizers as Oracles. As part of **RQ-3**, we evaluate three strong non-personalized summarizers, BigBird-Pegasus (Zaheer et al., 2020), SimCLS (Liu & Liu, 2021), and T5-base (Raffel et al., 2020), under the “oracle” protocol of Vansh et al. (2023). We replace each query document’s title with the user’s gold-reference title to inject the true preference cue. This assesses whether frozen models can exploit the cues to produce seemingly personalized outputs.

362

5 RESULTS AND OBSERVATIONS

372

We present results w.r.t the three RQs (Section 4). All results have a significance of $p < 0.05$.

374

5.1 WALK2PERS-ENCODER PREDICTION ACCURACY

376

RQ1 — Are MDH models sufficient? We observe that MDH baselines fail to anticipate user trajectories reliably. Short-memory neural encoders (NAML/NRMS/EBNR) hover at chance AUC

378
 379 **Table 2: RQ-1/2: Next b-node Prediction (PENS Dataset):** Details in Table 14; **Cross-task trans-**
 380 **ferability** on Sequential News Recommendation (MIND Dataset): App I.4, Table 17.

Category	Models	AUC	MRR	nDCG@5	nDCG@10
MDH based	NAML	0.498	0.001	0.0004	0.0007
	NRMS	<u>0.499</u>	0.0009	0.0002	0.0004
	EBNR	<u>0.499</u>	0.0009	0.0003	0.0005
	SMD (ours)	0.415	0.094	0.052	0.065
SWH based	AGD (ours)	0.446	0.113	0.069	0.073
	Walk2Pers-Encoder w/o Geometric Step (ours)	0.474	<u>0.121</u>	<u>0.082</u>	<u>0.132</u>
	Walk2Pers-Encoder Full (ours)	<u>0.532</u>	<u>0.23</u>	<u>0.198</u>	<u>0.249</u>

386
 387 **Table 3: (RQ-3:) Walk2Pers-Encoder Validation:** Personalized summarization performance
 388 (w.r.t PSE-JSD/SU-4/METEOR) comparison with SOTA baselines on the PENS dataset.

Category	Model	PSE-JSD	PSE-SU4	PSE-METEOR
Oracle Summarizers (via Cue Injection)	BigbirdPegasus	0.253	0.143	0.168
	SimCLS	0.157	0.032	0.116
	T5-base	0.073	0.011	0.022
LLMs (w/ 0-shot user history)	LLaMA-13B	0.187	0.069	0.078
	Zephyr-7B	0.211	0.081	0.089
	Mistral-7B	0.212	0.082	0.098
	DeepSeek-14B	0.152	0.078	0.084
LLMs (w/ 2-shot user history)	LLaMA-13B	0.227	0.078	0.081
	Zephyr-7B	0.231	0.085	0.086
	Mistral-7B	0.235	0.087	0.084
	DeepSeek-14B	0.248	0.094	0.097
LLMs (Prompt-chaining)	Qwen-3-23.5B	0.105	0.082	0.082
	Gemini-2.5-Flash	0.222	0.104	0.124
	Mistral-7B	0.072	0.026	0.023
	DeepSeek-14B	0.078	0.028	0.024
Fine-tuned Specialized (Personalized) ~ MDH	PENS-NAML-T1	0.021	0.014	0.016
	PENS-EBNR-T1	0.015	0.010	0.011
	PENS-EBNR-T2	0.011	0.008	0.009
	PENS-NRMS-T1	0.015	0.011	0.011
	PENS-NRMS-T2	0.008	0.007	0.007
	GTP	0.024	0.017	0.019
	SP-Individual	0.017	0.015	0.014
	SMD + T5-UCA-Decoder	0.143	0.136	0.107
	AGD + T5-UCA-Decoder	0.286	0.214	0.248
	– w/o Geometric Step + T5-UCA-Decoder	0.306	0.334	0.321
Markov Drift (MDH) Encoders (ours)	– Full + T5-C4-Decoder	<u>0.418</u>	<u>0.341</u>	<u>0.422</u>
	– Full + T5-UCA-Decoder	<u>0.452</u>	<u>0.383</u>	<u>0.449</u>

406 (≈ 0.5) and collapse on rank metrics ($\text{MRR} \leq 0.001$, $\text{nDCG} \leq 5 \times 10^{-4}$), showing that compressed
 407 hidden states carry little predictive signal. Among controlled variants, action gating helps (AGD >
 408 SMD, e.g., MRR 0.113 vs. 0.094), but overall accuracy remains low, as past signals vanish quickly
 409 and reinforcement/suppression is absent.

410 **RQ2 — Do SWH components yield systematic gains?** We find that adding dual memories
 411 and drift (Walk2Pers-Enc. w/o Geo) already surpasses the best baseline AGD (AUC +0.028,
 412 nDCG@10 +0.059). Geometric magnitude–orientation step yields large additional jumps (AGD:
 413 AUC +0.086 / +0.117 / +0.176 w.r.t AUC/MRR/nDCG@5/10). These results confirm that mem-
 414 ory lanes preserve reinforcement/suppression, while geometric steps capture continuity vs. novelty.

416 5.2 RQ-3: WALK2PERS END-TO-END SUMMARIZATION PERFORMANCE

417 To address **RQ3**, we benchmark Walk2Pers against the strong summarizer baselines as described
 418 in Section 4.2. Evaluation is conducted on PENS and OpenAI (Reddit) datasets and further validated
 419 using the PersonalSumm dataset using the three PerSEval metrics (PSE-JSD/SU4/METEOR), which
 420 correlate strongly with human preference ratings (Appendix A.2.1).

422 **Comparison with Specialized Personalized Summarizers.** We see that Walk2Pers consistently
 423 outperform all specialized models (Table 3). While SOTA frameworks like GTP and SP yield PSE
 424 scores in the 0.017–0.024 range, Walk2Pers achieves 0.452/0.383/0.449 (JSD/SU4/METEOR),
 425 corresponding to average absolute gains of 0.41 over these fine-tuned MDH instantiations. This
 426 highlights that explicit geometric-step modeling with dual memory lanes captures preference evolu-
 427 tion more effectively than both RNN- and Transformer-based encoders.

428 **Comparison with LLMs.** LLMs improve when conditioned with user histories. However, they
 429 remain substantially below Walk2Pers. For instance, the best two-shot configuration (DeepSeek-
 430 14B) is outperformed by Walk2Pers by margins of 0.20/0.29/0.35. On average, Walk2Pers
 431 yields gains of 0.22 across all LLMs (including long context models Gemini and Qwen3). Prompt-
 432 chaining is even less effective, falling behind even MDH baselines. Furthermore, evaluation on the

432
433
434
435
436
437
438

Table 4: (RQ-3) Cross-domain generalizability on OpenAI (Reddit)

Category	Model	PSE-JSD	PSE-SU4	PSE-METEOR
LLMs (w/ 2-shot user history)	LLaMA-13B	0.232	0.093	0.107
	Zephyr-7B	0.214	0.087	0.104
	Mistral-7B	0.226	0.088	0.103
	DeepSeek-14B	0.243	0.095	0.109
Walk2Pers	Full + T5-UCA-Decoder	0.339	0.303	0.350

Table 5: Personalized Summarization Performance w.r.t Human-Judgment Ratings: Avg. interpolated rating (w/ RMSD dist. from gold reference) on OpenAI (Reddit) dataset

Category	Model	RMSD (generated vs. gold reference)	HJ Rating
Fine-tuned Specialized (Personalized) ~ MDH	PENS+EBNR-T1	0.932	2
	PENS+EBNR-T2	0.938	2
	PENS+NAML-T1	0.926	2
	PENS+NRMS-T1	0.911	2
	PENS+NRMS-T2	0.919	2
	GTP+TrRMLo	0.939	2
	SP	0.881	3
Best-forming LLMs (w/ 2-shot user history)	Mistral	0.791	5
	Gemini	0.782	5
	DeepSeek	0.779	5
T5-UCA-Decoder + MDH Encoders	SMD	0.836	4
	AGD	0.701	6
SWH w/ T5-UCA-Decoder	Walk2Pers w/o Geometric Step	<u>0.461</u>	7
	Walk2Pers (Full)	<u>0.396</u>	7

OpenAI (Reddit) dataset (Table 4) confirms that **Walk2Pers** **indicates cross-domain generalization**, outperforming the strongest LLM baseline by 0.09/0.20/0.24 across JSD/SU4/METEOR. We also evaluate **Walk2Pers** on the translated PersonalSum dataset and observe scores of 0.31/0.28/0.3 w.r.t. PSE-JSD/SU4/METEOR, underscoring the efficacy in datasets tailored for personalized summarization. These results suggest that while prompting improves LLMs, it cannot substitute a dedicated action-aware encoder that explicitly models user trajectories.

Comparison with Oracle Summarizers. We observe that oracle summarizers, augmented with gold preference cues, fall short. BigBird-Pegasus, the strongest oracle, is outperformed by a margin of 0.20/0.24/0.28. Relative to SimCLS and T5-base, the margins are even larger (0.29/0.35/0.43 and 0.43/0.37/0.38, resp.). This underscores that **Walk2Pers** utilizes evolving preferences better than the best-possible performance of non-personalized architectures.

5.3 HUMAN-RATING GROUNDED EVALUATION

While RQ1/2 provide behavioral faithfulness against human trajectories, as a part of RQ-3, we complement this by assessing how generated summaries align with what users *prefer*. Using the multi-domain non-news OpenAI-Reddit dataset, which contains multiple (5781) human-rated summaries of 9 models for 642 query documents, we identify 1042 top-rated (i.e., 7) one per user as the *human-preferred reference*. We then measure the SBert-embedding-space RMSD-divergence of the model-generated summaries from the reference and create a ground rating-to-RMSD-range map table, where each rating row has its corresponding average min-max range. Using this table, we interpolate the HJ-rating of our baseline models as in Table 5. We observe that both full and w/o geometric step variants (trained on OpenAI-train) of **Walk2Pers** achieve an average rating of 7 out of 7, while MDH-models are significantly underperforming, with the exception of AGD. Interpolation computation details in Appendix I.1. We also report the standard accuracy metrics-based evaluation in Table 18.

6 CONCLUSION

In this paper, we contrast the *Markovian Drift Hypothesis* (MDH) with our proposed *Structured Walk Hypothesis* (SWH), which models preference evolution as an action-conditioned geometric walk with memory. **Walk2Pers**, our proposed instantiation of SWH, encodes trajectories through action-aware b-cells, dual memory lanes, and magnitude–orientation steps, balancing continuity with novelty. Experiments show that the next behavior (b-node) prediction, the primary test of SWH, outperforms MDH baselines. At the same time, downstream personalized summarization confirms that stronger preference modeling yields more user-aligned outputs. While limited by fixed memory kernels and reliance on limited noisy logs, **Walk2Pers** demonstrates that preference evolution is better framed as SWH than as shallow MDH.

486 CODE OF ETHICS STATEMENT
487

488 This research adheres to the ICLR Code of Ethics². In conducting this work, we: (i) contributed to
489 society and human well-being by advancing methods for trustworthy personalized summarization;
490 (ii) upheld high standards of scientific excellence through transparent reporting, reproducibility,
491 and acknowledgement of prior work; (iii) avoided harm by ensuring that our methods were tested
492 responsibly, with no foreseeable misuse to compromise safety, security, or privacy; (iv) were honest,
493 trustworthy, and transparent in disclosing our methods, limitations, and potential risks; (v) acted
494 fairly and without discrimination, considering inclusivity in data and evaluation; (vi) respected the
495 work and rights of others via proper citation and intellectual property compliance; and (vii) respected
496 privacy by not using personally identifiable or sensitive information in our datasets. (viii) used LLMs
497 (GPT-5) limited to structural changes (paraphrasing and summarization of our own content, which
498 has not been used verbatim in most of the paper), table format corrections, and extensive literature
499 review (using Deep Research). We have not used LLM for any content *generation* purpose.

500
501 REPRODUCIBILITY STATEMENT
502

503 We have made significant efforts to ensure the reproducibility of our work. All details of the pro-
504 posed Walk2Pers framework, including the encoder and decoder variants, training objectives, and
505 evaluation protocols, are provided in Sections 3.3 and 4. Hyperparameter choices, model configu-
506 rations, and training details are documented in Appendix H.2 and Table 13. Dataset descriptions,
507 preprocessing steps, and evaluation metrics (PSE-JSD, SU-4, METEOR) are clearly specified in
508 Section 2, Appendices C, A.2.1, and B. We also provide ablation studies (Tables 2 & 3) to demon-
509 strate robustness to design choices. To facilitate independent verification, we include a zip file of
510 our source code and scripts in the supplementary material, which allows reproduction of all reported
511 experiments.

512 REFERENCES
513

514 Elliot Anshelevich, Zack Fitzsimmons, Rohit Vaish, and Lirong Xia. Representative proxy vot-
515 ing. *Proceedings of the AAAI Conference on Artificial Intelligence*, 35(6):5086–5093, May
516 2021. doi: 10.1609/aaai.v35i6.16643. URL <https://ojs.aaai.org/index.php/AAAI/article/view/16643>.

518 Xiang Ao, Xiting Wang, Ling Luo, Ying Qiao, Qing He, and Xing Xie. PENS: A dataset and
519 generic framework for personalized news headline generation. In Chengqing Zong, Fei Xia,
520 Wenjie Li, and Roberto Navigli (eds.), *Proceedings of the 59th Annual Meeting of the As-
521 sociation for Computational Linguistics and the 11th International Joint Conference on Nat-
522 ural Language Processing (Volume 1: Long Papers)*, pp. 82–92, Online, August 2021. As-
523 sociation for Computational Linguistics. doi: 10.18653/v1/2021.acl-long.7. URL <https://aclanthology.org/2021.acl-long.7/>.

525 Klaudia Balcer and Piotr Lipinski. Session-based recommender systems: User interest as a stochas-
526 tic process in the latent space, 2025. URL <https://arxiv.org/abs/2504.10005>.

528 Satanjeev Banerjee and Alon Lavie. METEOR: An automatic metric for MT evaluation with
529 improved correlation with human judgments. In *Proceedings of the ACL Workshop on In-
530 trinsic and Extrinsic Evaluation Measures for Machine Translation and/or Summarization*, pp.
531 65–72, Ann Arbor, Michigan, June 2005. Association for Computational Linguistics. URL
532 <https://aclanthology.org/W05-0909>.

533 Pengshan Cai, Kaiqiang Song, Sangwoo Cho, Hongwei Wang, Xiaoyang Wang, Hong Yu, Fei
534 Liu, and Dong Yu. Generating user-engaging news headlines. In Anna Rogers, Jordan Boyd-
535 Gruber, and Naoaki Okazaki (eds.), *Proceedings of the 61st Annual Meeting of the Association
536 for Computational Linguistics (Volume 1: Long Papers)*, pp. 3265–3280, Toronto, Canada, July
537 2023. Association for Computational Linguistics. doi: 10.18653/v1/2023.acl-long.183. URL
538 <https://aclanthology.org/2023.acl-long.183/>.

539 ²<https://iclr.cc/public/CodeOfEthics>

540 Junsu Cho and Hyun. Dynamic multi-behavior sequence modeling for next item recommendation.
 541 In *Proceedings of the AAAI conference on artificial intelligence*, 2023.

542 Sourish Dasgupta, Ankush Chander, Tanmoy Chakraborty, Parth Borad, and Isha Motiyani. PerSE-
 543 val: Assessing personalization in text summarizers. *Transactions on Machine Learning Research*,
 544 2024. ISSN 2835-8856. URL <https://openreview.net/forum?id=yqT7eBz1VJ>.

545 DeepSeek-AI, Daya Guo, Dejian Yang, Haowei Zhang, Junxiao Song, Ruoyu Zhang, Runxin Xu,
 546 Qihao Zhu, Shirong Ma, Peiyi Wang, Xiao Bi, Xiaokang Zhang, Xingkai Yu, Yu Wu, Z. F. Wu,
 547 Zhibin Gou, Zhihong Shao, Zhuoshu Li, Ziyi Gao, Aixin Liu, Bing Xue, Bingxuan Wang, Bochao
 548 Wu, Bei Feng, Chengda Lu, Chenggang Zhao, and Chengqi et al. Deepseek-r1: Incentivizing
 549 reasoning capability in llms via reinforcement learning, 2025. URL <https://arxiv.org/abs/2501.12948>.

550 Zi-Yi Dou, Pengfei Liu, Hiroaki Hayashi, Zhengbao Jiang, and Graham Neubig. GSum: A general
 551 framework for guided neural abstractive summarization. In Kristina Toutanova, Anna Rumshisky,
 552 Luke Zettlemoyer, Dilek Hakkani-Tur, Iz Beltagy, Steven Bethard, Ryan Cotterell, Tanmoy
 553 Chakraborty, and Yichao Zhou (eds.), *Proceedings of the 2021 Conference of the North Ameri-
 554 can Chapter of the Association for Computational Linguistics: Human Language Technologies*,
 555 pp. 4830–4842, Online, June 2021. Association for Computational Linguistics. doi: 10.18653/v1/
 556 2021.naacl-main.384. URL [https://aclanthology.org/2021.naacl-main.384/](https://aclanthology.org/2021.naacl-main.384).

557 Abdul Ghafoor Etemad, Ali Imam Abidi, and Megha Chhabra. Fine-tuned t5 for abstractive sum-
 558 marization. *International Journal of Performability Engineering*, 17(10), 2021.

559 Angela Fan, Shruti Bhosale, Holger Schwenk, Zhiyi Ma, Ahmed El-Kishky, Siddharth Goyal, Man-
 560 deep Baines, Onur Celebi, Guillaume Wenzek, Vishrav Chaudhary, Naman Goyal, Tom Birch,
 561 Vitaliy Liptchinsky, Sergey Edunov, Edouard Grave, Michael Auli, and Armand Joulin. Beyond
 562 english-centric multilingual machine translation, 2020. URL <https://arxiv.org/abs/2010.11125>.

563 Junxian He, Wojciech Kryscinski, Bryan McCann, Nazneen Rajani, and Caiming Xiong. CTRL-
 564 sum: Towards generic controllable text summarization. In Yoav Goldberg, Zornitsa Kozareva,
 565 and Yue Zhang (eds.), *Proceedings of the 2022 Conference on Empirical Methods in Natu-
 566 ral Language Processing*, pp. 5879–5915, Abu Dhabi, United Arab Emirates, December 2022.
 567 Association for Computational Linguistics. doi: 10.18653/v1/2022.emnlp-main.396. URL
 568 <https://aclanthology.org/2022.emnlp-main.396/>.

569 Albert Q. Jiang, Alexandre Sablayrolles, Arthur Mensch, Chris Bamford, Devendra Singh Chap-
 570 lot, Diego de las Casas, Florian Bressand, Gianna Lengyel, Guillaume Lample, Lucile Saulnier,
 571 Lélio Renard Lavaud, Marie-Anne Lachaux, Pierre Stock, Teven Le Scao, Thibaut Lavril,
 572 Thomas Wang, Timothée Lacroix, and William El Sayed. Mistral 7b, 2023. URL <https://arxiv.org/abs/2310.06825>.

573 Frederic Kirstein, Terry Ruas, Robert Kratel, and Bela Gipp. Tell me what I need to know:
 574 Exploring LLM-based (personalized) abstractive multi-source meeting summarization. In
 575 Franck Dernoncourt, Daniel Preoțiuc-Pietro, and Anastasia Shimorina (eds.), *Proceedings of
 576 the 2024 Conference on Empirical Methods in Natural Language Processing: Industry Track*,
 577 pp. 920–939, Miami, Florida, US, November 2024. Association for Computational Linguistics.
 578 doi: 10.18653/v1/2024.emnlp-industry.69. URL <https://aclanthology.org/2024.emnlp-industry.69/>.

579 Srijan Kumar, Xikun Zhang, and Jure Leskovec. Predicting dynamic embedding trajectory in tem-
 580 poral interaction networks. In *Proceedings of the 25th ACM SIGKDD International Conference
 581 on Knowledge Discovery & Data Mining*, KDD ’19, pp. 1269–1278, New York, NY, USA, 2019a.
 582 Association for Computing Machinery. ISBN 9781450362016. doi: 10.1145/3292500.3330895.
 583 URL <https://doi.org/10.1145/3292500.3330895>.

584 Srijan Kumar, Xikun Zhang, and Jure Leskovec. Predicting dynamic embedding trajectory in tem-
 585 poral interaction networks. In *Proceedings of the 25th ACM SIGKDD International Conference
 586 on Knowledge Discovery & Data Mining*, KDD ’19, pp. 1269–1278, New York, NY, USA, 2019b.
 587 Association for Computing Machinery. ISBN 9781450362016. doi: 10.1145/3292500.3330895.
 588 URL <https://doi.org/10.1145/3292500.3330895>.

594 Alon Lavie and Abhaya Agarwal. Meteor: an automatic metric for mt evaluation with high levels
 595 of correlation with human judgments. In *Proceedings of the Second Workshop on Statistical*
 596 *Machine Translation*, StatMT '07, USA, 2007. Association for Computational Linguistics.

597

598 Mike Lewis, Yinhan Liu, Naman Goyal, Marjan Ghazvininejad, Abdelrahman Mohamed, Omer
 599 Levy, Veselin Stoyanov, and Luke Zettlemoyer. BART: Denoising sequence-to-sequence pre-
 600 training for natural language generation, translation, and comprehension. In *Proceedings of the*
 601 *58th Annual Meeting of the Association for Computational Linguistics*, pp. 7871–7880. Asso-
 602 ciation for Computational Linguistics, July 2020. doi: 10.18653/v1/2020.acl-main.703. URL
 603 <https://aclanthology.org/2020.acl-main.703>.

604 Zekun Li, Baolin Peng, Pengcheng He, Michel Galley, Jianfeng Gao, and Xifeng Yan. Guiding large
 605 language models via directional stimulus prompting. In *Proceedings of the 37th International*
 606 *Conference on Neural Information Processing Systems*, NIPS '23, Red Hook, NY, USA, 2023.
 607 Curran Associates Inc.

608 Junhong Lian, Xiang Ao, Xinyu Liu, Yang Liu, and Qing He. Panoramic interests: Stylistic-content
 609 aware personalized headline generation. In *Companion Proceedings of the ACM on Web Confer-*
 610 *ence 2025*, 2025.

611 Chin-Yew Lin. ROUGE: A package for automatic evaluation of summaries. In *Text Summarization*
 612 *Branches Out*, pp. 74–81, Barcelona, Spain, July 2004. Association for Computational Linguis-
 613 tics. URL <https://aclanthology.org/W04-1013>.

614

615 Nelson F. Liu, Kevin Lin, John Hewitt, Ashwin Paranjape, Michele Bevilacqua, Fabio Petroni, and
 616 Percy Liang. Lost in the middle: How language models use long contexts. *Transactions of the*
 617 *Association for Computational Linguistics*, 12:157–173, 2024. doi: 10.1162/tacl_a_00638. URL
 618 <https://aclanthology.org/2024.tacl-1.9/>.

619

620 Yixin Liu and Pengfei Liu. SimCLS: A simple framework for contrastive learning of abstractive
 621 summarization. In *Proceedings of the 59th Annual Meeting of the Association for Compu-
 622 tational Linguistics and the 11th International Joint Conference on Natural Language Processing*
 623 *(Volume 2: Short Papers)*, pp. 1065–1072. Association for Computational Linguistics, August
 624 2021. doi: 10.18653/v1/2021.acl-short.135. URL <https://aclanthology.org/2021.acl-short.135>.

625

626 M.L. Menéndez, J.A. Pardo, L. Pardo, and M.C. Pardo. The jensen-shannon divergence. *Jour-
 627 nal of the Franklin Institute*, 334(2):307–318, 1997. ISSN 0016-0032. doi: [https://doi.org/10.1016/S0016-0032\(96\)00063-4](https://doi.org/10.1016/S0016-0032(96)00063-4). URL <https://www.sciencedirect.com/science/article/pii/S0016003296000634>.

628

629 Shumpei Okura, Yukihiro Tagami, Shingo Ono, and Akira Tajima. Embedding-based news
 630 recommendation for millions of users. In *Proceedings of the 23rd ACM SIGKDD Interna-
 631 tional Conference on Knowledge Discovery and Data Mining*, KDD '17, pp. 1933–1942, New
 632 York, NY, USA, 2017. Association for Computing Machinery. ISBN 9781450348874. doi:
 633 10.1145/3097983.3098108. URL <https://doi.org/10.1145/3097983.3098108>.

634

635 Zhonghong Ou, Xiao Zhang, and Zhu. Ls-tgnn: Long and short-term temporal graph neural net-
 636 work for session-based recommendation. In *Proceedings of the AAAI Conference on Artificial*
 637 *Intelligence*, 2025.

638

639 Zhe Pan and Peng Wang. Hyperbolic hierarchy-aware knowledge graph embedding for link pre-
 640 diction. In Marie-Francine Moens, Xuanjing Huang, Lucia Specia, and Scott Wen-tau Yih
 641 (eds.), *Findings of the Association for Computational Linguistics: EMNLP 2021*, pp. 2941–2948,
 642 Punta Cana, Dominican Republic, November 2021. Association for Computational Linguistics.
 643 doi: 10.18653/v1/2021.findings-emnlp.251. URL [https://aclanthology.org/2021.findings-emnlp.251/](https://aclanthology.org/2021.findings-emnlp.251).

644

645 Divya Patel, Pathik Patel, Ankush Chander, Sourish Dasgupta, and Tanmoy Chakraborty. Are large
 646 language models in-context personalized summarizers? get an iCOPERNICUS test done! In
 647 Yaser Al-Onaizan, Mohit Bansal, and Yun-Nung Chen (eds.), *Proceedings of the 2024 Conference*
 648 *on Empirical Methods in Natural Language Processing*, pp. 16820–16842, Miami, Florida, USA,

648 November 2024. Association for Computational Linguistics. doi: 10.18653/v1/2024.emnlp-main.
 649 935. URL <https://aclanthology.org/2024.emnlp-main.935/>.

650

651 Jie Qiu, Yifan Zhang, Zhichao Hou, Xiangnan He, Tong Xu, and Xing Xie. S-walk: Accurate and
 652 scalable session-based recommendation with random walks. In *Proceedings of the 15th ACM*
 653 *International Conference on Web Search and Data Mining (WSDM)*, pp. 88–96, New York, NY,
 654 USA, 2022. ACM. doi: 10.1145/3488560.3498442.

655 Colin Raffel, Noam Shazeer, Adam Roberts, Katherine Lee, Sharan Narang, Michael Matena, Yanqi
 656 Zhou, Wei Li, and Peter J. Liu. Exploring the limits of transfer learning with a unified text-to-
 657 text transformer. *Journal of Machine Learning Research*, 21(140):1–67, 2020. URL <http://jmlr.org/papers/v21/20-074.html>.

658

659 GS Ramesh, Vamsi Manyam, Vijoosh Mandula, Pavan Myana, Sathvika Macha, and Suprith Reddy.
 660 Abstractive text summarization using t5 architecture. In *Proceedings of Second International*
 661 *Conference on Advances in Computer Engineering and Communication Systems: ICACECS*
 662 2021, pp. 535–543. Springer, 2022.

663

664 Nils Reimers and Iryna Gurevych. Sentence-bert: Sentence embeddings using siamese bert-
 665 networks. In *Proceedings of the 2019 Conference on Empirical Methods in Natural Language*
 666 *Processing*. Association for Computational Linguistics, 11 2019. URL <https://arxiv.org/abs/1908.10084>.

667

668 Yun-Zhu Song, Yi-Syuan Chen, Lu Wang, and Hong-Han Shuai. General then personal: De-
 669 coupling and pre-training for personalized headline generation. *Transactions of the Association*
 670 *for Computational Linguistics*, 11:1588–1607, 2023. doi: 10.1162/tacl_a_00621. URL
 671 <https://aclanthology.org/2023.tacl-1.90/>.

672

673 Zhiqing Sun, Zhi-Hong Deng, Jian-Yun Nie, and Jian Tang. Rotate: Knowledge graph embedding by
 674 relational rotation in complex space. In *International Conference on Learning Representations*,
 675 2019. URL <https://openreview.net/forum?id=HkgEQnRqYQ>.

676

677 T Tawmo, Mrinmoi Bohra, Pankaj Dadure, Partha Pakray, et al. Comparative analysis of
 678 t5 model for abstractive text summarization on different datasets. In *Proceedings of the*
 679 *International Conference on Innovative Computing Communication (ICICC) 2022*. SSRN,
 680 2022. URL <https://ssrn.com/abstract=4096413> or <http://dx.doi.org/10.2139/ssrn.4096413>.

681

682 Qwen Team. Qwen3 technical report, 2025. URL <https://arxiv.org/abs/2505.09388>.

683

684 Hanghang Tong, Christos Faloutsos, and Jia-Yu Pan. Fast Random Walk with Restart and its Ap-
 685 plications. In *Proceedings of the Sixth International Conference on Data Mining (ICDM)*, pp.
 686 613–622, Washington, DC, USA, 2006. IEEE Computer Society. doi: 10.1109/ICDM.2006.70.

687

688 Hugo Touvron, Louis Martin, Kevin Stone, Peter Albert, Amjad Almahairi, Yasmine Babaei, Niko-
 689 lay Bashlykov, Soumya Batra, Prajjwal Bhargava, Shruti Bhosale, et al. Llama 2: Open founda-
 690 tion and fine-tuned chat models. *arXiv e-prints*, pp. arXiv–2307, 2023.

691

692 Lewis Tunstall, Edward Beeching, Nathan Lambert, Nazneen Rajani, Kashif Rasul, Younes Belkada,
 693 Shengyi Huang, Leandro von Werra, Clémentine Fourrier, Nathan Habib, et al. Zephyr: Direct
 694 distillation of lm alignment. *arXiv e-prints*, pp. arXiv–2310, 2023.

695

696 Rahul Vansh, Darsh Rank, Sourish Dasgupta, and Tanmoy Chakraborty. Accuracy is not enough:
 697 Evaluating personalization in summarizers. In *Findings of the Association for Compu-
 698 tational Linguistics: EMNLP 2023*, pp. 2582–2595, Singapore, December 2023. Association
 699 for Computational Linguistics. doi: 10.18653/v1/2023.findings-emnlp.169. URL <https://aclanthology.org/2023.findings-emnlp.169>.

700

701 Michael Völske, Martin Potthast, Shahbaz Syed, and Benno Stein. TL;DR: Mining Reddit to
 702 learn automatic summarization. In Lu Wang, Jackie Chi Kit Cheung, Giuseppe Carenini,
 703 and Fei Liu (eds.), *Proceedings of the Workshop on New Frontiers in Summarization*, pp. 59–
 704 63, Copenhagen, Denmark, September 2017. Association for Computational Linguistics. doi:
 705 10.18653/v1/W17-4508. URL <https://aclanthology.org/W17-4508>.

702 Chuhan Wu, Fangzhao Wu, Mingxiao An, Jianqiang Huang, Yongfeng Huang, and Xing Xie. Neural
 703 news recommendation with attentive multi-view learning. In *Proceedings of the Twenty-Eighth*
 704 *International Joint Conference on Artificial Intelligence*. International Joint Conferences on Arti-
 705 *ficial Intelligence Organization*, 2019a.

706 Chuhan Wu, Fangzhao Wu, Suyu Ge, Tao Qi, Yongfeng Huang, and Xing Xie. Neural news rec-
 707 ommendation with multi-head self-attention. In *Proceedings of the 2019 Conference on Em-
 708 pirical Methods in Natural Language Processing and the 9th International Joint Conference on
 709 Natural Language Processing (EMNLP-IJCNLP)*, pp. 6389–6394, Hong Kong, China, Novem-
 710 ber 2019b. Association for Computational Linguistics. doi: 10.18653/v1/D19-1671. URL
 711 <https://aclanthology.org/D19-1671>.

712 Fangzhao Wu, Ying Qiao, Jiun-Hung Chen, Chuhan Wu, Tao Qi, Jianxun Lian, Danyang Liu, Xing
 713 Xie, Jianfeng Gao, Winnie Wu, and Ming Zhou. MIND: A large-scale dataset for news recom-
 714 mendation. In Dan Jurafsky, Joyce Chai, Natalie Schluter, and Joel Tetreault (eds.), *Proceedings*
 715 *of the 58th Annual Meeting of the Association for Computational Linguistics*, pp. 3597–3606, On-
 716 line, July 2020. Association for Computational Linguistics. doi: 10.18653/v1/2020.acl-main.331.
 717 URL <https://aclanthology.org/2020.acl-main.331>.

718 Wen Xiao, Yujia Xie, Giuseppe Carenini, and Pengcheng He. Personalized abstractive summariza-
 719 tion by tri-agent generation pipeline. In Yvette Graham and Matthew Purver (eds.), *Findings*
 720 *of the Association for Computational Linguistics: EACL 2024*, pp. 570–581, St. Julian’s, Malta,
 721 March 2024. Association for Computational Linguistics. URL <https://aclanthology.org/2024.findings-eacl.39/>.

722 Manzil Zaheer, Guru Guruganesh, Kumar Avinava Dubey, Joshua Ainslie, Chris Alberti, Santi-
 723 ago Ontanon, Philip Pham, Anirudh Ravula, Qifan Wang, Li Yang, and Amr Ahmed. Big bird:
 724 Transformers for longer sequences. In *Advances in Neural Information Processing Systems*, vol-
 725 ume 33, pp. 17283–17297, 2020. URL https://proceedings.neurips.cc/paper_files/paper/2020/file/c8512d142a2d849725f31a9a7a361ab9-Paper.pdf.

726 Lemei Zhang, Peng Liu, Marcus Tiedemann Oakland Henriksboe, Even W. Lauvral, Jon Atle
 727 Gulla, and Heri Ramampiaro. Personalsum: A user-subjective guided personalized summariza-
 728 tion dataset for large language models. In *The Thirty-eight Conference on Neural Information
 729 Processing Systems Datasets and Benchmarks Track*, 2024. URL <https://openreview.net/forum?id=ETZk7lqyaF>.

730 Wei Zhang, Xiaoyu Li, Chen Sun, Hongzhi Wang, and Yongfeng Zhang. D-rdw: Diversity-driven
 731 random walks for news recommendation. In *Proceedings of the ACM Web Conference (WWW)*,
 732 New York, NY, USA, 2025. ACM. To appear.

733 Zhanqiu Zhang, Jianyu Cai, Yongdong Zhang, and Jie Wang. Learning hierarchy-aware knowl-
 734 edge graph embeddings for link prediction. In *Proceedings of the AAAI conference on artificial*
 735 *intelligence*, volume 34, pp. 3065–3072, 2020.

736 Xiaoyu Zhu, Chenyang Bu, Bingbing Dong, Shengwei Ji, Yi He, and Xindong Wu. Ikgn: Intention-
 737 aware knowledge graph network for poi recommendation. In *2023 IEEE International Conference*
 738 *on Data Mining (ICDM)*, pp. 908–917, 2023. doi: 10.1109/ICDM58522.2023.00100.

739

740

741

742

743

744

745

746 **A MEASURING DEGREE-OF-PERSONALIZATION**

747

748 **A.1 MOTIVATION**

749

750 Vansh et al. (2023) proposed EGISES— a metric to measure the degree of **insensitivity-to-**
 751 **subjectivity** for relative benchmarking of how much models *lack personalization* (i.e., a lower
 752 score is better within the range $[0, 1]$) instead of assigning an absolute goodness score. Based on
 753 this notion, they defined (summary-level) “**deviation**” of a model $M_{\theta, u}$ (later termed as **Degree-of-**
 754 **Responsiveness** (DEGRESS) by Dasgupta et al. (2024)) as follows:

755 **Summary-level DEGRESS.** Given a document d_i and a user-profile u_{ij} (user j ’s ex-
 756 pected summary), the summary-level responsiveness of a personalized model $M_{\theta, u}$, (i.e.,

756 DEGRESS($s_{u_{ij}} | (d_i, u_{ij})$), is defined as the *proportional* divergence between model-generated summary 757 $s_{u_{ij}}$ of d_i for j -th user from other user-specific summary versions w.r.t a corresponding divergence 758 of u_{ij} from the other user-profiles.

759 DEGRESS($s_{u_{ij}} | (d_i, u_{ij})$) is formulated as:

$$\begin{aligned}
 760 \text{DEGRESS}(&s_{u_{ij}} | (d_i, u_{ij})) = \frac{1}{|\mathbf{U}_{d_i}|} \sum_{k=1}^{|\mathbf{U}_{d_i}|} \frac{\min(X_{ijk}, Y_{ijk}) + \epsilon}{\max(X_{ijk}, Y_{ijk}) + \epsilon} \\
 761 X_{ijk} = \frac{\exp(w(u_{ij}|u_{ik}))}{\sum_{l=1}^{|\mathbf{U}_{d_i}|} \exp(w(u_{ij}|u_{il}))} \cdot \sigma(u_{ij}, u_{ik}); \quad Y_{ijk} = \frac{\exp(w(s_{u_{ij}}|s_{u_{ik}}))}{\sum_{l=1}^{|\mathbf{U}_{d_i}|} \exp(w(s_{u_{ij}}|s_{u_{il}}))} \cdot \sigma(s_{u_{ij}}, s_{u_{ik}}) \\
 762 w(u_{ij}|u_{ik}) = \frac{\sigma(u_{ij}, u_{ik})}{\sigma(u_{ij}, d_i)}; \quad w(s_{u_{ij}}|s_{u_{ik}}) = \frac{\sigma(s_{u_{ij}}, s_{u_{ik}})}{\sigma(s_{u_{ij}}, d_i)}
 \end{aligned} \quad (6)$$

770 Here, $|\mathbf{D}|$ is the total number of documents in the evaluation dataset, $|\mathbf{U}|$ is the total number of 771 users who created gold-reference summaries that reflect their expected summaries (and thereby, 772 their subjective preferences), and $|\mathbf{U}_{d_i}| (= |\mathbf{S}_{d_i}|)$ is the number of users who created gold-references 773 for document d_i . w is the divergence of the model-generated summary $s_{u_{ij}}$ (and the corresponding 774 expected summary u_{ij}) from document d_i itself in comparison to all the other versions. It 775 helps to determine how much percentage (therefore, the softmax function) of the divergence (i.e., 776 $\sigma(s_{u_{ij}}, s_{u_{ik}})$) should be considered for the calculation of DEGRESS. If $s_{u_{ij}}$ is farther than $s_{u_{ik}}$ w.r.t d_i 777 then $\text{DEGRESS}(s_{u_{ij}} | (d_i, u_{ij})) < \text{DEGRESS}(s_{u_{ik}} | (d_i, u_{ik}))$, implying that $M_{\theta, u}$ is more responsive 778 to the k -th reader. A lower value of $\text{DEGRESS}(s_{u_{ij}} | (d_i, u_{ij}))$ indicates that while reader-profiles 779 are different, the generated summary $s_{u_{ij}}$ is very similar to other reader-specific summaries (or vice 780 versa), and hence, is not responsive at the summary-level. The system-level DEGRESS and EGISES 781 have been formulated as follows:

$$\text{DEGRESS}(M_{\theta, u}) = \frac{\sum_{i=1}^{|\mathbf{D}|} \frac{\sum_{j=1}^{|\mathbf{U}_{d_i}|} \text{DEGRESS}(s_{u_{ij}} | (d_i, u_{ij}))}{|\mathbf{U}_{d_i}|}}{|\mathbf{D}|} \quad (7)$$

A.2 PERSEVAL: FORMULATION

786 As can be noted, the **DEGRESS formualtion does not enforce any penalty on accuracy drop**. To 787 rectify this Dasgupta et al. (2024) proposed PerSEval. The design of PerSEval had two key 788 goals: (i) to penalize models for poor accuracy, while simultaneously (ii) ensuring that the evaluation 789 of responsiveness (i.e., DEGRESS) is not overshadowed by high accuracy. This penalty is referred to 790 as the **Effective DEGRESS Penalty Factor (EDP)**. If a model achieves 100% accuracy, no EDP will 791 be applied, and the PerSEval score will equal the DEGRESS score. The following formulation 792 of PerSEval guarantees these properties:

$$\begin{aligned}
 793 \text{PerSEval}(s_{u_{ij}} | (d_i, u_{ij})) &= \text{DEGRESS}(s_{u_{ij}} | (d_i, u_{ij})) \times \text{EDP}(s_{u_{ij}} | (d_i, u_{ij})) \\
 794 \text{where, } \text{EDP}(s_{u_{ij}} | (d_i, u_{ij})) &= 1 - \frac{1}{1 + 10^{\alpha \geq 3} \cdot \exp(-10^{\beta \geq 1} \cdot \text{DGP}(s_{u_{ij}} | (d_i, u_{ij})))}, \\
 795 \text{DGP}(s_{u_{ij}} | (d_i, u_{ij})) &= \text{ADP}(s_{u_{i*}} | (d_i, u_{i*})) + \text{ACP}(s_{u_{ij}} | (d_i, u_{ij}))
 \end{aligned} \quad (8)$$

800 Here, ADP is a document-level penalty due to a drop in accuracy for the best-performance of the 801 model (i.e., the model-generated summary of document d_i ($s_{u_{i*}}$) is closest to the corresponding 802 reader's expected summary u_{ij}). ADP is formulated as follows:

$$\begin{aligned}
 803 \text{ADP}(s_{u_{i*}} | (d_i, u_{i*})) &= \frac{1}{1 + 10^{\gamma \geq 4} \cdot \exp\left(-10 \cdot \frac{\sigma^*(s_{u_{i*}}, u_{i*})|d_i - \mathbf{0}}{(1 - \sigma^*(s_{u_{i*}}, u_{i*})|d_i) + \epsilon}\right)} \\
 804 \text{where, } \sigma^*(s_{u_{i*}}, u_{i*})|d_i &= \min_{j=1}^{|\mathbf{U}_{d_i}|} \sigma(s_{u_{ij}}, u_{ij})|d_i
 \end{aligned} \quad (9)$$

805 and $\{\epsilon : \text{An infinitesimally small number} \in (0, 1)\}$

810 ADP ensures that even if the DEGRESS score is acceptable, a penalty due to accuracy drop can
 811 still be imposed as a part of EDP. ADP, however, fails to address the scenario where the best-case
 812 scenario is acceptable (i.e., accuracy is fairly high) but is rather an outlier case – i.e., for most of
 813 the other model-generated summary versions, there is a considerable accuracy drop. To address
 814 this issue, the second penalty component within EDP called *Accuracy-inconsistency Penalty* (ACP)
 815 was introduced which evaluates whether a model consistently performs w.r.t accuracy for a specific
 816 generated summary compared to its average performance. ACP is formulated as:

$$817 \quad \text{ACP}(s_{u_{ij}} | (d_i, u_{ij})) = \frac{1}{1 + 10^{\gamma \geq 4} \cdot \exp \left(-10 \cdot \frac{\sigma(s_{u_{ij}}, u_{ij}) | d_i - \sigma^*(s_{u_{i\bullet}}, u_{i\bullet}) | d_i}{(\bar{\sigma}(s_{u_{i\bullet}}, u_{i\bullet}) | d_i - \sigma^*(s_{u_{i\bullet}}, u_{i\bullet}) | d_i) + \epsilon} \right)} \quad (10)$$

$$820 \quad \text{where, } \bar{\sigma}(s_{u_{i\bullet}}, u_{i\bullet}) | d_i = \frac{1}{|\mathbf{U}_{d_i}|} \sum_{j=1}^{|\mathbf{U}_{d_i}|} \sigma(s_{u_{ij}}, u_{ij}) | d_i$$

823 The system-level PerSEval score is as follows:

$$825 \quad \text{PerSEval}(M_{\theta, u}) = \frac{\sum_{i=1}^{|\mathbf{D}|} \frac{\sum_{j=1}^{|\mathbf{U}_{d_i}|} \text{PerSEval}(s_{u_{ij}} | (d_i, u_{ij}))}{|\mathbf{U}_{d_i}|}}{|\mathbf{D}|} \quad (11)$$

830 The system-level PerSEval $\in [0, 1]$ and is bounded by the system-level DEGRESS score.

832 A.2.1 PSE METRICS

833 **PerSEval-RG-SU4** (or PSE-SU4) is the PerSEval variant that uses ROUGE-SU4 (Lin, 2004)
 834 as a distance metric (i.e., σ) in the PerSEval formula. PSE-SU4 has been reported to have high
 835 human-judgment correlation (Pearson’s r : 0.6; Spearman’s ρ : 0.6; Kendall’s τ : 0.51) Dasgupta et al.
 836 (2024). The **ROUGE-SU4** score is based on *skip-bigrams*, which are pairs of words that appear in
 837 the same order within a sentence but can have up to four other words between them. The formula is
 838 as follows:

839 For a given generated summary G and reference summary R , the ROUGE-SU4 score is calculated
 840 as:

842 **Skip-Bigram Recall** (R_{SU4}):

$$843 \quad R_{SU4} = \frac{\text{Count of matching skip-bigrams between } G \text{ and } R}{\text{Total skip-bigrams in } R}$$

846 **Skip-Bigram Precision** (P_{SU4}):

$$848 \quad P_{SU4} = \frac{\text{Count of matching skip-bigrams between } G \text{ and } R}{\text{Total skip-bigrams in } G}$$

851 **F1 Score** ($F1_{SU4}$): The F1 score is the harmonic mean of precision and recall:

$$854 \quad F1_{SU4} = \frac{2 \times P_{SU4} \times R_{SU4}}{P_{SU4} + R_{SU4}}$$

856 Where:

- 859 • A **skip-bigram** consists of two words in the correct order but with zero to four words
 860 skipped in between.
- 861 • Matching skip-bigrams are counted between the generated summary and the reference sum-
 862 mary.

863 The final **ROUGE-SU4** score is typically reported as the F1 measure, balancing precision and recall.

864 **PerSEval-JSD** (or PSE-JSD) is the PerSEval variant that uses the Jensen–Shannon Diver-
 865 gence (JSD) (Menéndez et al., 1997) as the distance metric σ in the PerSEval formula. JSD is a
 866 smoothed and symmetric version of Kullback–Leibler divergence between the unigram (or n-gram)
 867 distributions of the generated summary G and reference summary R . Its formulation is:
 868

$$869 \quad \text{JSD}(P \parallel Q) = \frac{1}{2} \text{KL}(P \parallel M) + \frac{1}{2} \text{KL}(Q \parallel M) \quad \text{where } M = \frac{1}{2}(P + Q) \quad (12)$$

871 here, P and Q are the normalized n-gram probability distributions of G and R respectively, and
 872

$$873 \quad \text{KL}(P \parallel M) = \sum_x P(x) \log \frac{P(x)}{M(x)}.$$

876 We then define the divergence as: $\sigma_{\text{JSD}}(G, R) = \text{JSD}(P_G \parallel P_R)$ and plug σ_{JSD} into all occurrences
 877 of σ in Equations equation 6–equation 11 to obtain PSE-JSD.

879 **PerSEval-Meteor** (or PSE-Meteor) uses the METEOR score Banerjee & Lavie (2005); Lavie &
 880 Agarwal (2007) as the similarity metric; we convert it into a distance by $1 - \text{METEOR}$. METEOR
 881 aligns unigrams (with synonymy, stem, and paraphrase matching) and combines precision, recall,
 882 and a fragmentation penalty. Its formulation is:
 883

$$884 \quad P = \frac{|\text{matched_unigrams}|}{|\text{unigrams}(G)|}, \quad R = \frac{|\text{matched_unigrams}|}{|\text{unigrams}(R)|}, \quad (13)$$

$$887 \quad F_\alpha = \frac{P R}{\alpha P + (1 - \alpha) R}, \quad \alpha \in [0, 1], \quad (14)$$

$$889 \quad \text{Penalty} = \gamma \left(\frac{\#\text{chunks}}{|\text{matched_unigrams}|} \right)^\beta, \quad \gamma, \beta > 0, \quad (15)$$

$$892 \quad \text{METEOR}(G, R) = (1 - \text{Penalty}) \times F_\alpha. \quad (16)$$

894 We then set $\sigma_{\text{Meteor}}(G, R) = 1 - \text{METEOR}(G, R)$, and substitute σ_{Meteor} for σ in Equations
 895 equation 6–equation 11 to yield PSE-Meteor.
 896

898 B PREDICTION METRICS

900 In this section, we provide definitions of the evaluation metrics used in our experiments: *AUC*, *MRR*,
 901 and *nDCG@k*. Each metric captures a complementary aspect of ranking quality when comparing
 902 the predicted next-step positions against the ground-truth target.

904 **Area Under Curve (AUC)** AUC measures how well the model ranks the ground-truth item rela-
 905 tive to all other candidates. Formally, if r is the rank (1-based) of the ground-truth item among C
 906 candidates, we define:

$$907 \quad \text{AUC} = \frac{C - r}{C - 1}.$$

909 This normalizes the rank to the interval $[0, 1]$, where higher values indicate that the true item is
 910 ranked closer to the top. Intuitively, AUC reflects the overall discriminative ability of the model.

912 **Mean Reciprocal Rank (MRR)** MRR emphasizes how highly the correct item appears in the
 913 ranked list. Given the rank r of the ground-truth item, its reciprocal rank is:

$$914 \quad \text{RR} = \frac{1}{r}.$$

917 MRR is the average of RR values across all queries. MRR rewards systems that consistently place
 the true item very close to the top of the ranking.

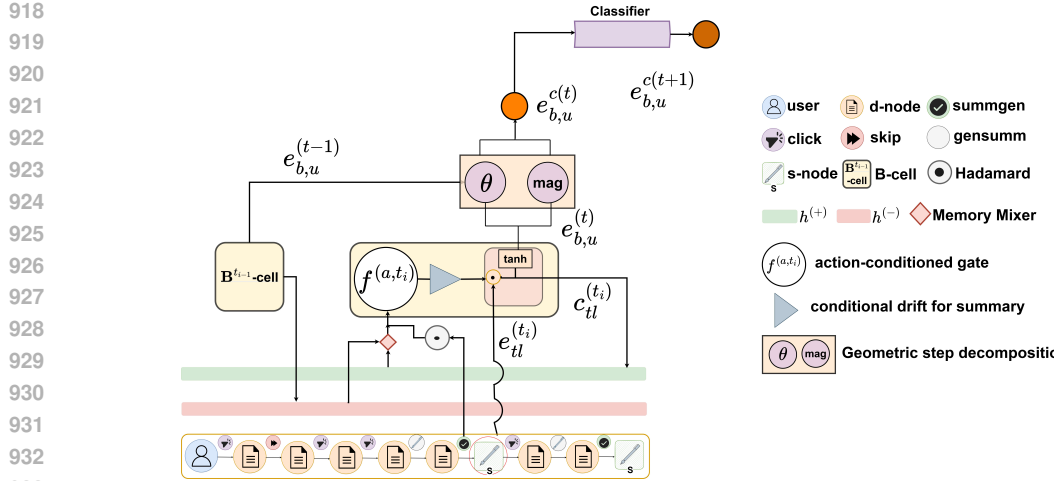


Figure 2: **Walk2Pers-Encoder**: The **b-cell** generates a b-node embedding $e_{b,u}^{(t)}$ at timestep t using the tail-node embedding $e_{tl}^{(t)}$, the action embedding $e_a^{(t)}$, and the history $h^{(t-1)}$ from the previous tail-cell content $c_{tl}^{(t-1)}$ (inside the corresponding b-cell); $c_{tl}^{(t-1)}$ updates the **dual memory lanes** (h^+, h^-) that persists positive (*click, summarize*) and negative (*skip*) memory resp. to create a **mixed history** $h^{(t-1)}$ which in turn is modulated by a **action-specific gate** $f^{(a,t)}$ and a conditional *summGen*-action-triggered **drift** (Δ) before fusing with the tail-node $e_{tl}^{(t)}$; the generated $e_{b,u}^{(t)}$ then goes through a **geometric-step decomposer** to re-orient the embedding w.r.t continuity vs. novelty.

Normalized Discounted Cumulative Gain (nDCG@k) nDCG@k evaluates the quality of the top- k predictions, with stronger weight on higher-ranked positions. The gain of a relevant item at rank r is discounted logarithmically:

$$\text{DCG}@k = \sum_{i=1}^k \frac{\mathbb{I}\{r_i = \text{target}\}}{\log_2(1+i)},$$

where $\mathbb{I}\{\cdot\}$ is an indicator function. Since there is only one relevant target per query, DCG@ k reduces to $\frac{1}{\log_2(1+r)}$ if the target appears within the top- k , and 0 otherwise. Normalization divides by the best possible score (which is 1 if the target is at rank 1). Thus:

$$\text{nDCG}@k = \begin{cases} \frac{1}{\log_2(1+r)}, & \text{if } r \leq k, \\ 0, & \text{otherwise.} \end{cases}$$

nDCG@ k highlights whether the correct prediction is placed near the very top of the model’s candidate list.

These three metrics together provide a comprehensive evaluation: AUC captures global rank discrimination, MRR emphasizes early precision, and nDCG@ k measures the quality of the truncated top- k predictions.

C DATASETS

C.1 PENS DATASET

The PENS dataset (Ao et al., 2021) includes 113,762 news articles across 15 topics. Each article contains an ID, title (avg. 10.5 words), body (avg. 549 words), and category, with titles linked to WikiData entities. The dataset also includes user interaction data, such as impressions and click behaviors, combined with news bodies and headlines from the MIND dataset Wu et al. (2020).

PENS training set. For training, 500k user-news impressions were sampled from June 13 to July 3, 2019. Each log records user interaction as [uID, tmp, clkNews, uclkNews, clkedHis], where

972

973

974

975

976

977

978

979

980

981

982

983

984

985

986

987

988

989

990

991

992

993

994

995

996

997

998

999

1000

1001

1002

1003

1004

1005

1006

1007

1008

1009

1010

1011

1012

1013

1014

1015

1016

1017

1018

1019

1020

1021

1022

1023

1024

1025

Table 6: MS/CAS PENS Dataset and Interaction Statistics

Characteristic	Dimension	Value
Article Stats		
General Stats	# Topics	15
	# Articles	113,762
	Avg. Title Length	10.5 words
	Avg. Body Length	549 words
Train Dataset Statistics		
Interaction Data	# User–News Impressions (anon.)	500,000
	# Users (anon.)	445,000
	Time Period	June 13–July 3, 2019
	User Interaction Fields	[uID, tmp, clkNews, uclkNews, clkedHis]
Test Dataset Statistics		
Participant Stats	# Participants	103
	Participant Category	English-speaking college students
	# Articles	3,940
	Browsed Headlines (Click + Skip)	1,000 per participant
Gold Reference (Participant-written Headlines)	Min. Interested (Click) Headlines	50 per participant
	Summarized Article Bodies	200 per participant
	Avg. Summaries per Article	4

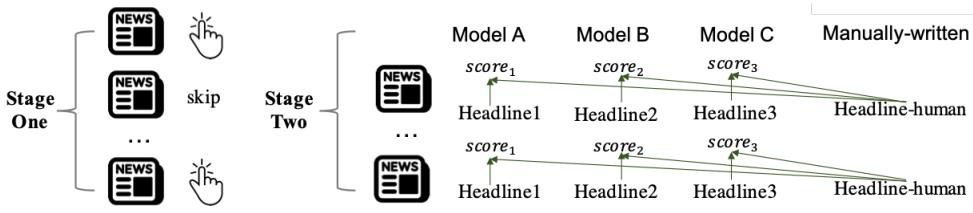


Figure 3: Stages of creation of testing dataset consisting of personalized headlines

‘clkNews’ and ‘uclkNews’ represent clicked and unclicked news, and ‘clkedHis’ refers to the user’s prior clicked articles, sorted by click time. The training data for `Walk2Pers`, as discussed in Section 4.1, shows high preference shift. This inherently supports that personalizing UX is strongly dependent on the temporal dynamics of the user. The stats are in the table 6.

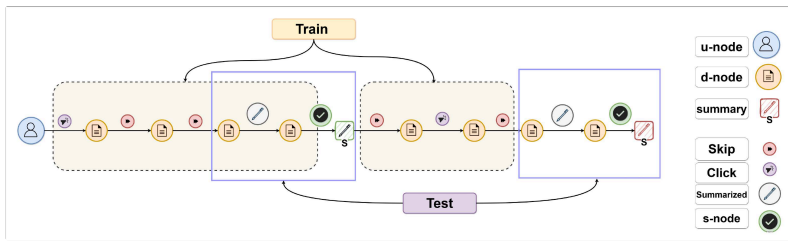
PENS test set. To create an offline testbed, 103 English-speaking students reviewed 1,000 headlines in stage-1, and then selected 50 articles, and created preferred headlines (i.e., expected gold-reference summaries) for 200 unseen articles in stage-2 (see Figure 3). Each article was reviewed by four participants. Editors checked for factual accuracy, discarding incorrect headlines. The high-quality remaining headlines serve as personalized gold-standard references in the PENS dataset.

C.2 OPENAI (REDDIT) DATASET

The OpenAI (Reddit) dataset (Völske et al., 2017) comprises 123,169 Reddit posts collected from 29 distinct subreddits. This dataset provides both OpenAI-generated and human-written summaries and is organized into two splits: Comparisons, used for training and validation, and Axis, designated for validation and testing. A curated subset of 1,038 posts was processed by 13 different summarization policies, resulting in the generation of 7,713 summaries. These summaries underwent evaluation by 64 annotators who rated paired summaries based on selection preferences, confidence in their ratings, and dimensions such as accuracy, coherence, coverage, and overall quality. Notably, unlike datasets like PENS, these summaries are not linked to individual annotators or their reading histories, which means they lack elements of personalization and contextual user information. Stats are in Table 7

1026
1027
1028
1029
1030
1031
1032
1033
1034
1035
1036
1037
1038
1039
1040
1041
1042
1043
1044
1045
1046
1047
1048
1049
1050
1051
1052
1053
1054
1055
1056
1057
1058
1059
1060
1061
1062
1063
1064
1065
1066
1067
1068
1069
1070
1071
1072
1073
1074
1075
1076
1077
1078
1079
Table 7: OpenAI TL;DR (Reddit) Dataset Statistics

Characteristic	Dimension	Value
Dataset Overview		
General Stats	# Reddit Posts	123,169
	# Subreddits (Domains)	29
	Policy-Generated Summaries	115,579
	Human-Written Summaries Available	
Train + Validation Dataset Statistics		
Article Stats	# Reddit Posts	21,111
	# Policies	81
	# Generated Summaries	107,866
	# Annotators	76
Subset Details	# Summary-Pairs Rated	64,832
	Validation Subset Statistics	
	# Reddit Posts	1,038
	# Policies	13
Evaluation Stats	# Generated Summaries	7,713
	# Annotators	32
	Test Dataset (RLHF-Tuned Policies) Statistics	
	# Evaluated Policies	4
Feedback Collection	# Evaluated Reddit Posts	57 (out of 1,038)
	Evaluation Method	Indirect Benchmarking
Annotation and Feedback		
Feedback Collection	Rating Scale	1–7
	Confidence Scale	1–9
	Avg. Ratings per Annotator	1,176
	Annotation Format	Summary-Pairs Selection

Figure 4: **UIG Construction:** Construction of User-Interaction Graph from preference datasets.

C.3 PERSONALSUM DATASET

The PersonalSum dataset (Zhang et al., 2024) is a crowd-annotated benchmark designed for personalized summarization. It consists of 441 Norwegian news articles across diverse topics and a total of 1,099 human-written summaries contributed by 39 unique annotators. Each article is paired with a GPT-4-generated generic summary (post-edited by students for fluency and factuality), and on average, 3 personalized summaries, written by crowdworkers to reflect their individual preferences and topical interests. Annotators also highlight the source sentences from the article that informed their summaries, adding explicit grounding for each summary segment.

PersonalSum annotation process. The dataset was constructed in three stages. In Stage-1, a GPT-4-generated generic summary was created for each article, refined by human editors, and tagged with sentence-level source highlights. In Stage-2, crowdworkers were recruited to write summaries from a personal perspective. Each worker completed comprehension questions and highlighted source text, ensuring fidelity to the original article. In Stage-3, automatic quality checks using GPT-3.5-based scoring (evaluating coherence, relevance, and consistency) filtered poor-quality annotations. Only those scoring above a threshold were retained. The final dataset comprises high-quality user-personalized summaries with source alignments and user metadata anonymized for privacy.

C.4 UIG CONSTRUCTION

To construct a User-Interaction Graph (UIG) from preference datasets, we distinguish between two types: (i) trajectory-based datasets like PENS Ao et al. (2021), which directly encode user inter-

1080
1081 **Table 8: PersonalSum Dataset Statistics**
1082

Characteristic	Dimension	Value
Dataset Overview		
General Stats	# Articles	441
	# Annotators	39
	# Personalized Summaries	1,099
	Avg. Personalized Summaries per Article	~3
Summary Types		
Summary Stats	GPT-4 Generic Summaries (Post-edited)	441
	Human-Personalized Summaries	1,099
	Avg. Summaries per Annotator	~28
Annotation Process		
Stages	Stage-1: Generic Summary Creation	GPT-4 → Human Editing + Highlights
	Stage-2: Personalized Summarization	Crowdworkers + Source Highlighting
	Stage-3: Quality Filtering	GPT-3.5 Scoring (Coherence, Relevance, Consistency)
	Final Dataset	High-quality, aligned summaries with anonymized metadata
Annotation Details		
Feedback and Grounding	Source Sentence Highlighting	Yes
	Comprehension Questions	Yes
	User Metadata	Anonymized

1097 **Table 9: User-Interaction Graph Statistics** for our $\mathcal{T}_{\text{train}}^{\text{PENS-D}}$, $\mathcal{T}_{\text{train}}^{\text{OAI}}$ and $\mathcal{T}_{\text{train}}^{\text{PS-EN}}$.
1098

Characteristic	$\mathcal{T}_{\text{train}}^{\text{PENS-D}}$	$\mathcal{T}_{\text{train}}^{\text{OAI}}$	$\mathcal{T}_{\text{train}}^{\text{PS-EN}}$
# u-nodes (trajectories)	55,000	18,000	700
# d-nodes per trajectory	134	39	17
# s-nodes per trajectory	15	12	4
Average trajectory length	143	47	23
# Max. trajectory length	200	50	32
# Min. trajectory length	5	25	7
Rate of Topic Shift	0.77	0.48	0.41

1107 actions, and (ii) feedback-based datasets like OpenAI-Reddit Völske et al. (2017), which lack user
1108 trajectories but contain document nodes (d-nodes), model-generated summaries (s-nodes), and sub-
1109 jective user feedback (e.g., ratings with confidence scores). For PENS-style datasets, we first build a
1110 trajectory pool \mathcal{T}^P using click and skip interactions (e.g., *clkNews* and *uclkNews*), but this yields an
1111 incomplete user profile due to the absence of personalized s-nodes. To address this, we augment \mathcal{T}^P
1112 with s-nodes from the test set by inserting `summarize` and `summGen` edges at the appropriate time
1113 steps, resulting in a derived pool \mathcal{T}^{P-D} . For OpenAI-style datasets, we infer preference sequences by
1114 classifying d-nodes as clicked if any associated system-generated summary received a rating above
1115 a threshold (i.e., greater than equals to 6 out of 9), then selecting the highest-rated summary as a
1116 surrogate s-node. The UIG construction algorithm is described in Algorithm 1.

D THEORETICAL ANALYSIS: SWH STRICTLY GENERALIZES MDH

1120 We provide formal derivations showing that the Structured Walk Hypothesis (SWH) strictly gener-
1121 alizes the Markovian Drift Hypothesis (MDH).

1122 **Lemma D.1** (Reduction: SWH recovers MDH). *For any MDH update of the form*

$$1124 e_{b,u}^{(t+1)} = f(e_{b,u}^{(t)}, a^{(t)}, q) + \epsilon^{(t)}, \quad \epsilon^{(t)} \sim \mathcal{N}(0, \Sigma(a^{(t)})),$$

1125 *there exists a parameter setting of SWH (Eq. 3) that reproduces it.*

1127 *Proof.* Set $\Psi \equiv 0$ and $\delta \equiv 0$. The increment under MDH is $\Delta e^{(t)} = f(e_{b,u}^{(t)}, a^{(t)}, q) - e_{b,u}^{(t)}$. We
1128 can select $u^{(t)} = \Delta e^{(t)} / \|\Delta e^{(t)}\|$, any $o^{(t)} \perp u^{(t)}$, and set $\text{mag}(a^{(t)})$ to $\text{mag}(a^{(t)}) = \|\Delta e^{(t)}\|$,
1129 $\theta(a^{(t)}) = 0$. Then $\Phi = \Delta e^{(t)}$, and Eq. 3 collapses to the MDH update. Noise $\epsilon^{(t)}$ is matched by
1130 sampling mag or adding a Gaussian head tied to $a^{(t)}$. \square

1132 **Corollary D.2** (MDH variants as special cases). *The following well-known models are recovered as
1133 degenerate cases of SWH:*

1134 **Algorithm 1** UIG Construction

1135 0: **function** CONSTRUCT_UIG(train, test_data, type)

1136 1: Initialize $\mathcal{T}_{\text{PENS}}, \mathcal{T}_{\text{OAI}} \leftarrow \emptyset$

1137 2: **for** each user u in train_data **do**

1138 3: Initialize $\tau^u \leftarrow \emptyset$

1139 4: **for** each interaction in u 's data **do**

1140 5: **if** type = PENS **then**

1141 6: Map to d-node with a *click/skip* edge based on interaction

1142 7: **else**

1143 8: Map to d-node with *click/skip* edge based on rating

1144 9: **if** rating confidence = max **then**

1145 10: Map to d-node with *gensum*, and s-node with *sumgen* edge

1146 11: **end if**

1147 12: **end if**

1148 13: Append mapped d-node to τ^u

1149 14: **end for**

1150 15: Add τ^u to $\mathcal{T}_{\text{PENS}}$ or \mathcal{T}_{OAI} based on type

1151 16: **end for**

1152 17: **if** type = PENS **then**

1153 18: **for** τ^u in $\mathcal{T}_{\text{PENS}}$ **do**

1154 19: Retrieve and insert s-nodes from test_data using *genSumm/sumgen* edges

1155 20: **end for**

1156 21: **return** $\mathcal{T}^{\text{PENS-D}} \leftarrow \mathcal{T}_{\text{PENS}}$

1157 22: **else**

1158 23: **return** \mathcal{T}_{OAI}

1159 24: **end if**

1160 24: **end function**=0

1161 • **Pure Random Walk (PRW):** $\text{mag} = 0, \Psi = 0, \delta = 0$.

1162 • **Action-aware Random Walk (ARW):** Same as PRW, but with action-conditioned noise $\epsilon^{(t)} \sim \mathcal{N}(0, \Sigma(a^{(t)}))$.

1163 • **Random Walk with Restart (RWR):** Tong *et al.* (2006) proposed this popular diffusion model

1164 where, at each step, the walk either (i) follows the graph transition with probability $(1 - \alpha)$ or (ii)

1165 “restarts” to a fixed seed distribution q with probability α . This ensures the walk remains centered

1166 around the most recent interaction and does not drift arbitrarily far. In our SWH framework, this

1167 corresponds to choosing $\Phi = \alpha(q - e_{b,u}^{(t)})$ with $\theta = 0$ and $\alpha \in (0, 1)$.

1168 **Lemma D.3** (Short-memory encoders are contained). Any continuous short-memory update

1169 $\tilde{f}(e_{b,u}^{(t)}, a^{(t)})$ (e.g., GRU, attention block) is realizable by SWH with $\Psi = \delta = 0$, since $\Phi =$

1170 $\tilde{f}(e_{b,u}^{(t)}, a^{(t)}) - e_{b,u}^{(t)}$.

1171 **Theorem D.4** (Strict Generalization). SWH strictly generalizes MDH:

1172 1. Every MDH update is realizable by SWH (Lemmas D.1–D.2).

1173 2. There exist SWH updates that no MDH update can reproduce.

1174 *Proof.* (i) follows from the lemmas. (ii) Consider two histories $\mathcal{H}_1, \mathcal{H}_2$ with identical $(e_{b,u}^{(t)}, a^{(t)})$ but

1175 distinct memories (h_t^+, h_t^-) . Eq. 3 yields increments $\Phi + \Psi(h_t^+, h_t^-) + \delta$ and $\Phi + \Psi(h_t'^+, h_t'^-) + \delta$,

1176 which differ. Since MDH is first-order Markov in $(e_{b,u}^{(t)}, a^{(t)}, q)$, it cannot separate \mathcal{H}_1 from \mathcal{H}_2 .

1177 Thus SWH has strictly greater expressivity. \square

1178 **Corollary D.5** (Non-Markovianity from dual memory). If Ψ aggregates asymmetric signals over

1179 multiple timesteps, the resulting process is non-Markovian with respect to the pair $(e_{b,u}^{(t)}, a^{(t)})$, and

1180 hence lies outside the scope of MDH.

1188

1189
1190
Table 10: **Encoder Models are Markovian Drifters**: Walk2Pers uniquely integrates all aspects
of SWH; *history capped by context length; no persistent memory across examples.

Models	History	Memory	Action Conditioning	Explicit Step	Long-term Persistent Memory	Interpretability
Oracles (BigBird-Pegasus, SimCLS, T5-base)	✗	✗	✗ (gold injected as cues)	✗	✗	✗
LLMs (Zephyr, Mistral, LLaMA-2, DeepSeek)	✓ (injected in prompt)	✗	✗*	✗	✗	✗
PRW	✓	✗	✗	✗	✗	✗
SMD (Short-Memory Drift) (ours)	✓	✗	✓	✗	✗	✗
ARW	✓	✗	✓	✗	✗	✗
RWR / D-RDW	✓	✗	✓	✗	✗	✗
AGD (Action-Gated Drift) (ours)	✓	✗	✓	✗	✗	✗
NAML	✓	✗ (short)	✗	✗	✗	✗
NRMS	✓	✓ (short)	✓	✗	✗	✗
EBNR	✓	✓ (short)	✓	✗	✗	✗
GTP (w/ TrRMIo)	✓	✓ (injected short)	✓	✗	✗	✗
SP (Signature-Phrase)	✓	✓ (phrases)	✓	✗	✗	✗
Walk2Pers (ours)	✓	✓ (dual)	✓	✓	✓	✓

1191

1192
1193
1194
1195
1196
1197
Proof Sketch. Under MDH (Eq. 1), the next state depends only on the *current* preference embedding $e_{b,u}^{(t)}$ and action $a^{(t)}$. Thus two different histories \mathcal{H}_1 and \mathcal{H}_2 that lead to the same $(e_{b,u}^{(t)}, a^{(t)})$ are indistinguishable. In contrast, SWH retains separate reinforcement and suppression traces via dual memories (h_t^+, h_t^-) . If \mathcal{H}_1 contains repeated clicks on climate policy and \mathcal{H}_2 contains repeated skips of celebrity news, both may yield the same $e_{b,u}^{(t)}$, although (h_t^+, h_t^-) differ. Consequently, $\Psi(h_t^+, h_t^-)$ produces distinct updates in Eq. 3. Therefore the transition distribution $P(e_{b,u}^{(t+1)} | e_{b,u}^{(t)}, a^{(t)}, \mathcal{H}_i)$ depends on the full history \mathcal{H}_i , not just the present state, violating the Markov property. \square

1198

1199
1200
1201
1202
1203
1204
1205
1206
1207
Remark. This shows that even when the visible preference embedding $e_{b,u}^{(t)}$ is the same, Walk2Pers can differentiate users with distinct long-term interaction traces. This is impossible under MDH, where all memory beyond the latest step is collapsed into q . In other words, SWH reduces to MDH when memory and drift are disabled, but enables trajectories to diverge even when current states coincide. This matches the empirical evidence that user preferences depend on long-horizon, action-specific dynamics (see Table 3).

1214

E BASELINES

1215

E.1 BASELINES FOR RQ-1/2: TESTING MDH VS. SWH COMPONENTS

1216

1217
1218
1219
1220
1221
1222
To evaluate whether the Markovian Drift Hypothesis (MDH) suffices or if the Structured Walk Hypothesis (SWH) is necessary, we compare Walk2Pers against a suite of encoder variants and established news recommendation encoders:

1223

Short-Memory Gate (SMD). This is the minimal baseline consistent with the Markovian Drift Hypothesis. At timestep t_i , the update depends only on the immediate tail state and current action embedding via a convex gate:

1224

$$c_{tl}^{(t_i)} = \tanh(f_{SMD}^{(a,t_i)}) \odot e_{tl}^{(t_i)}, \quad e_{b,u}^{(t_i)} = \tanh(W_b c_{tl}^{(t_i)}),$$

1225

1226
1227
1228
1229
1230
1231
1232
where the gate is defined as: $f_{SMD}^{(a,t_i)} = \eta(W_a \cdot e_a^{(t_i)}) + (1 - \eta)(W_h \cdot c_{tl}^{(t_{i-1})})$. Here, $\eta \in (0, 1)$ is a learnable scalar which balances the contribution of the action embedding $e_a^{(t_i)}$ and the prior tail state $c_{tl}^{(t_{i-1})}$. Because this update overwrites history at each step, it carries no mechanism for reinforcement, suppression, or geometric decomposition, and thus strictly follows the MDH assumption.

1233

1234
1235
1236
1237
Action-Specific Gates (AGD). Instead of a generic convex combination, each action has its own parameterization of $f(\cdot)$. We design $f^{(a,t_i)}$ separately for *click*, *skip*, *summarize*, and *summGen*, so that each action boosts, mutes, or rebalances user interests. A *click* encodes positive reinforcement, implemented as a history-aware gain:

1238

$$f^{(clk,t_i)} = (\mathbf{W}_{clk} \cdot \mathbf{e}_{clk}^{(t_i)}) \odot \mathbf{c}_{tl}^{(t_{i-1})}, \quad \mathbf{c}_{tl}^{(t_i)} = \tanh(f^{(clk,t_i)}) \odot \mathbf{e}_{tl}^{(t_i)}. \quad (17)$$

1239

1240
1241
If Alice clicks on “Concert in New York”, the gain reinforces music-related features in her history. In contrast, *skip* reflects either disinterest in the current document or *pull* toward an alternative. In terms of the timesteps of the trajectory τ_u , this would be a look-ahead to timestep t_{i+1} where $\mathbf{c}_{tl}^{(t_i)}$

1242 is compared with $\mathbf{e}_{tl}^{(t_{i+1})}$ via a dot product $\langle \cdot \rangle$. We model this alternative attraction towards a more
 1243 preferred (in contrast to disinterest) alternative as a deviation $\eta_{attr}^{(t_i)}$:
 1244

$$1245 \quad f^{(skp, t_i)} = \tanh(\mathbf{W}_{skp} \mathbf{e}_{skp}^{(t_i)} + \mathbf{g}_{move}^{(t_i)}) \odot \mathbf{e}_{tl}^{(t_i)}; \text{ where: } \mathbf{g}_{move}^{(t_i)} = \lambda_1^{(t_i)} \mathbf{e}_{tl}^{(t_i)} + \mathbf{W}_{pull} \cdot \lambda_2^{(t_i)} \eta_{attr}^{(t_i)}; \quad (18)$$

$$1246 \quad \eta_{attr}^{(t_i)} = \max(\langle \mathbf{c}_{tl}^{(t_{i-1})}, \mathbf{e}_{tl}^{(t_{i+1})} \rangle, 1 - \langle \mathbf{c}_{tl}^{(t_{i-1})}, \mathbf{e}_{tl}^{(t_i)} \rangle); \mathbf{c}_{tl}^{(t_i)} = \tanh(f^{(skp, t_i)}) \odot \mathbf{e}_{tl}^{(t_i)}$$

$$1247$$

$$1248$$

1249 Here, $\mathbf{g}_{move}^{(t_i)}$ non-linearly distorts the trajectory. λ_1, λ_2 are learnable constants. To illustrate, Al-
 1250 ice may choose to skip a *Election Policies* article (due to disinterest) or leave, say “*Music During*
 1251 *Cooking*”, for a more preferred “*Latest Concerts by Pink Panther*” (i.e., the future pull).
 1252

1253 A summary request, i.e. `summarize` indicates focused intent anchored in the title of the document:
 1254

$$1254 \quad f^{(summ, t_i)} = (\mathbf{W}_{summ} \cdot \mathbf{e}_{summ}^{(t_i)}) \odot \mathbf{c}_{tl}^{(t_{i-1})}, \quad \mathbf{c}_{tl}^{(t_i)} = \tanh(f^{(summ, t_i)}) \odot \mathbf{e}_{title(tl)}^{(t_i)}. \quad (19)$$

$$1255$$

1256 Finally, generated summary `summGen` evaluates whether the summary is concise in terms of expec-
 1257 tations and faithful to the source content:
 1258

$$1259 \quad f^{(summGen, t_i)} = -\gamma \log \left(\exp(\mathbf{g}_{summGen} \odot \mathbf{e}_{tl}^{(t_i)}) + \exp((1 - \mathbf{g}_{summGen}) \odot \mathbf{e}_{tl}^{(t_{i-1})}) \right),$$

$$1260 \quad \mathbf{c}_{tl}^{(t_i)} = \tanh(f^{(summGen, t_i)}) \odot \mathbf{c}_{tl}^{(t_{i-1})}, \quad \mathbf{g}_{summGen} = \sigma(\mathbf{W}_{min}(\mathbf{W}_{summGen} \cdot \mathbf{e}_{summGen}^{(t_i)})). \quad (20)$$

$$1261$$

$$1262$$

1263 The gate $\mathbf{g}_{summGen}$ balances coverage of the source along with history alignment, with a learnable γ
 1264 tuning the trade-off between them. We generalize the gates as: $f^{(a, t_i)} = \text{AGD}(\mathbf{e}_a, t_i) \odot \mathbf{e}_{history}$,
 1265 where AGD determines which function to trigger based on the action a and $\mathbf{e}_{history}$ is the embedding
 1266 of the previous state history.
 1267

1268 E.2 BASELINES FOR RQ-3 (PERSONALIZED SUMMARIZATION PERFORMANCE)

1269 For downstream evaluation on personalized summarization, we compare against three categories of
 1270 strong baselines:
 1271

1272 E.2.1 BASELINE PERSONALIZED MODELS

1273 **PENS-NRMS Injection-Type 1.** The PENS framework (Ao et al., 2021) generates personalized
 1274 summaries by incorporating user embeddings along with the input news article. For this variant,
 1275 user embeddings are derived using NRMS (Neural News Recommendation with Multi-Head Self-
 1276 Attention) (Wu et al., 2019b), which includes a multi-head self-attention based news encoder to
 1277 represent news titles, and a user encoder that captures browsing behavior through multi-head self-
 1278 attention over clicked articles. Additive attention mechanisms are employed to highlight important
 1279 words and articles. In Injection-Type 1, the NRMS user embedding is injected by initializing the
 1280 decoder’s hidden state, thereby directly influencing the summary generation process from the start.
 1281

1282 **PENS-NRMS Injection-Type 2.** This variant also uses NRMS for user embedding, but personal-
 1283 ization is introduced differently. Instead of initializing the decoder, the user embedding is injected
 1284 into the attention mechanism of the PENS model. This modulates the attention weights over the
 1285 news body, enabling the model to focus on content aligned with the user’s preferences.
 1286

1287 **PENS-NAML Injection-Type 1.** NAML (Neural News Recommendation with Attentive Multi-
 1288 View Learning) (Wu et al., 2019a) generates news representations by attending over multiple views,
 1289 including titles, bodies, and topic categories. The user encoder learns from interacted news and
 1290 selects the most informative content for personalization. The resulting user embedding is integrated
 1291 into the PENS decoder using Injection-Type 1, i.e., by initializing the decoder’s hidden state.
 1292

1293 **PENS-EBNR Injection-Type 1.** EBNR (Embedding-based News Recommendation) (Okura
 1294 et al., 2017) models user preferences using an RNN over browsing histories to produce user em-
 1295 beddings. These embeddings are injected into the PENS model via Injection-Type 1 by initializing
 1296 the decoder, thereby influencing the initial decoding steps with user-specific information.
 1297

1296 **PENS-EBNR Injection-Type 2.** This configuration uses the same user encoder from EBNR but
 1297 applies Injection-Type 2. Here, the user embedding is incorporated into the decoder’s attention
 1298 layers, allowing the model to personalize attention distributions over the news body during decoding.
 1299

1300 **General Then Personal (GTP).** General Then Personal (GTP) (Song et al., 2023) is a two-stage
 1301 framework for personalized headline generation. In stage-1, a Transformer-based encoder-decoder
 1302 model is pre-trained on large-scale news article-headline pairs to learn robust, content-focused head-
 1303 line generation without personalization. In stage-2, a separate “headline customizer” refines the gen-
 1304 eral headline by incorporating user-specific preferences, which are encoded as a control code by the
 1305 user encoder TrRMIO. To bridge the gap between general generation and personalized refinement,
 1306 GTP introduces two mechanisms: (i) **Information Self-Boosting (ISB)**, which reintroduces relevant
 1307 content details from the article to prevent information loss during customization; and (ii) **Masked**
 1308 **User Modeling (MUM)**, which randomly masks parts of the user embedding during training and
 1309 reconstructs them, reducing the model’s over-reliance on its general parameters.

1310 **Signature Phrase.** Another line of personalization focuses on condensing a user’s reading history
 1311 into a collection of *signature phrases* (Cai et al., 2023). These phrases, derived through contrastive
 1312 learning over news articles without annotated data, act as dynamic user profiles that adapt as interests
 1313 evolve. Such phrases need not appear verbatim in the user’s history but instead encode higher-level
 1314 signals. Using these phrases, the model learns to generate personalized headlines that connect new
 1315 articles with the user’s inferred interests, yielding outputs that are engaging, relevant, and grounded
 1316 in article content rather than drifting toward clickbait.

1317 These encoders serve as competitive MDH-aligned baselines, since they reduce trajectories into
 1318 compressed short-term embeddings with no explicit long-term reinforcement or novelty modeling.
 1319

1320 E.2.2 BASELINE LLMs

1322 **Zephyr 7B β .** Zephyr(Tunstall et al., 2023) is a 7 billion parameter transformer model fine tuned
 1323 from Mistral 7 billion using Direct Preference Optimization on publicly available and synthetic data.
 1324 It removes traditional alignment constraints to improve raw performance and achieves strong results
 1325 on benchmarks such as MT Bench where it reports a score of 7.34 in comparison with 6.86 for
 1326 LLaMA 2-70B Chat. Zephyr is optimized for helpful dialogue and is openly available under an
 1327 MIT license. It focuses on efficiency and high quality responses without relying on reinforcement
 1328 learning from human feedback. The model supports an input context length of 32K tokens.

1329 **Mistral 7B.** Mistral Instruct(Jiang et al., 2023) is a dense transformer model that uses grouped
 1330 query attention and sliding window attention to efficiently scale with long context inputs. It is
 1331 pretrained on approximately two trillion tokens and provides strong performance across natural lan-
 1332 guage and code generation benchmarks, surpassing models such as LLaMA 2-13B in many evalua-
 1333 tions. Mistral Instruct is fully open source under the Apache 2.0 license and includes an instruction
 1334 tuned variant that is widely adopted for fine tuning and deployment. The model supports an input
 1335 context length of 32K tokens.

1337 **LLaMA 2 13B.** LLaMA two(Touvron et al., 2023) 13 billion by Meta is an autoregressive trans-
 1338 former trained on two trillion tokens of public data with a context length of 4096 tokens. It sup-
 1339 ports chat interaction through instruction tuning and reinforcement learning from human feedback.
 1340 Although originally state of the art among open models, it is surpassed in many tasks by newer ar-
 1341 chitectures such as Mistral-7 billion. LLaMA-2 remains an influential and widely used foundation
 1342 model with extensive documentation and open access under the Meta license.

1344 **DeepSeek R1 14B.** DeepSeek R1(DeepSeek-AI et al., 2025) is a 14.8 billion parameter model dis-
 1345 tilled from Qwen-2.5 14 billion and is designed for strong performance on mathematical reasoning,
 1346 coding, and multi step logical tasks. It is fine tuned on eight hundred thousand examples gener-
 1347 ated by a larger DeepSeek R1 model and is released under an MIT license. Despite its moderate
 1348 size, it rivals substantially larger models on benchmarks such as AIME and MATH while remaining
 1349 efficient for customization and deployment. The model supports an input context length of 128K
 tokens.

1350
1351 Gemini 2.5 Flash. Gemini-2.5 Flash is a compact and highly optimized member of the Gemini
1352 family designed for fast inference, large scale retrieval augmented generation, and multimodal in-
1353 teraction. It provides high throughput generation with reduced latency and is suitable for production
1354 applications that require consistent responsiveness. Gemini 2.5 Flash incorporates the same unified
1355 multimodal architecture used across the Gemini series and has been trained on a large mixture of
1356 text, code, and image data. The model supports an input context length of 1 million tokens, making
1357 it particularly effective for long document synthesis and extended conversational sessions.
1358

1359
1360 Qwen 3 235B. Qwen-2 235 billion is a large scale frontier transformer model developed as part of
1361 the Qwen three family. It is trained on extensive multilingual and multimodal datasets with a focus
1362 on reasoning, tool use, and high fidelity generation. The model is designed for advanced analytical
1363 tasks, multi hop reasoning, and instruction following at very high capability levels. Qwen-3 serves
1364 as a foundation for many distilled and specialized variants and is openly available for research and
1365 commercial use under a permissive license. The model supports an input context length of 256K,
1366 allowing it to operate effectively on extremely long sequences in both textual and mixed modality
1367 settings.
1368

1369 E.2.3 BASELINE GENERIC SUMMARIZERS

1370
1371 BigBirdPegasus. BigbirdPegasus, proposed by (Zaheer et al., 2020) is an extension of Trans-
1372 former based models designed specifically for processing longer sequences. It utilizes sparse atten-
1373 tion, global attention, and random attention mechanisms to approximate full attention. This enables
1374 BigBird to handle longer contexts more efficiently and, therefore, can be suitable for summarization.
1375

1376
1377 SimCLS. A Simple Framework for Contrastive Learning of Abstractive Summarization (Liu &
1378 Liu, 2021) uses a two-stage training procedure. In the first stage, a Seq2Seq model (Lewis et al.,
1379 2020) is trained to generate candidate summaries with MLE loss. Next, the evaluation model, initiated
1380 with RoBERTa is trained to rank the generated candidates with contrastive learning.
1381

1382
1383 T5. (Text-To-Text Transfer Transformer) is based on the Transformer-based Encoder-Decoder ar-
1384 chitecture that operates on the principle of the unified text-to-text task for any NLP problem, includ-
1385 ing summarization. Some recent analyses on the performance of T5 on summarization tasks can be
1386 found in (Raffel et al., 2020; Tawmo et al., 2022; Ramesh et al., 2022; Etemad et al., 2021).
1387

1388 F LICENSE AND USAGE STATEMENT

1389
1390 In this work, we utilize the following pre-trained large language models (LLMs): DeepSeek-R1 14B
1391 (MIT License), Mistral-7B-Instruct (Apache 2.0), LLaMA2-13B (Llama 2 Community License),
1392 and Zephyr 7B (β) (MIT License). All models are used according to their respective licenses and
1393 terms provided by their original creators. Proper attribution is given to each model’s developers as
1394 cited in our references. We also use the following datasets:
1395

- 1396 • **MS/CAS PENS dataset:** We comply with the dataset’s terms of use, which is de-
1397 rived from the Microsoft Research License ([https://github.com/msnews/MIND/
1398 blob/master/MSR%20License_Data.pdf](https://github.com/msnews/MIND/blob/master/MSR%20License_Data.pdf)).
- 1399 • **OpenAI Reddit dataset:** We comply with the MIT License specifications as set
1400 by OpenAI ([https://github.com/openai/summarize-from-feedback/
1401 blob/master/LICENSE](https://github.com/openai/summarize-from-feedback/blob/master/LICENSE))

1402 We have ensured that all datasets and models are used responsibly, respecting privacy, consent,
1403 and ethical guidelines. When applicable, data is anonymized and handled according to the ethical
1404 standards set forth by NeurIPS.

1404 **G WALK2PERS ARCHITECTURAL DETAILS**
 1405

1406 **G.1 WALK2PERS-ENCODER ARCHITECTURAL DETAILS**
 1407

1408 **Magnitude and Orientation Computation.** To capture the *direction* and *magnitude* of movement
 1409 in a complex embedding-based manifold, we proposed a geometrical walk of behaviors 3.3.1. This
 1410 walk conceptualizes preference evolution as a sequence of *directed steps* in semantic space where
 1411 each behavior is obtained by rotating and scaling the previous embedding to get the geometrically
 1412 contextualized $\mathbf{e}_{\mathbf{c}_{b_{u_j}}}^{(t_i)}$. We compute the **orientation degree of the update** as follows:
 1413

$$\begin{aligned} \theta^{(t_i)} &= \pi \cdot \tanh\left(\mathbf{W}_\theta \sigma(\mathbf{W}_{\text{angle}} \mathbf{e}_{b,u}^{(t_{i-1})})\right); o^{(t_i)} = \frac{v^{(t_i)} - \langle v^{(t_i)}, u^{(t_{i-1})} \rangle u^{(t_{i-1})}}{\max(\|v^{(t_i)} - \langle v^{(t_i)}, u^{(t_{i-1})} \rangle u^{(t_{i-1})}\|_2, \varepsilon)}, \\ v^{(t_i)} &= \frac{\mathbf{e}_{b,u}^{(t_i)} - \mathbf{e}_{b,u}^{(t_{i-1})}}{\max(\|\mathbf{e}_{b,u}^{(t_i)} - \mathbf{e}_{b,u}^{(t_{i-1})}\|_2, \varepsilon)}; u^{(t_{i-1})} = \frac{\mathbf{e}_{b,u}^{(t_i)}}{\max(\|\mathbf{e}_{b,u}^{(t_i)}\|_2, \varepsilon)}. \end{aligned} \quad (21)$$

1420 The angle $\theta^{(t_i)} \in (-\pi, \pi)$ serves as a *directional drift controller*, deciding whether the trajectory
 1421 should continue smoothly (small $\theta^{(t_i)}$) or shift sharply (large $\theta^{(t_i)}$). The vector $u^{(t_{i-1})}$ represents
 1422 the *forward direction* inherited from past context (carrying forward the momentum of current flow
 1423 of history), while $o^{(t_i)}$ denotes the *orthogonal novelty axis* derived from the raw transition direction
 1424 $v^{(t_i)}$. For example, if Alice has consistently read *Climate Science Articles*, $u^{(t_{i-1})}$ encodes this
 1425 momentum, while a sudden click on a *Policy Debate* yields a transition vector with a strong orthogonal
 1426 component $o^{(t_i)}$; a small $\theta^{(t_i)}$ implies smooth thematic extension (science into policy), whereas a
 1427 large $\theta^{(t_i)}$ reflects a sharp diffusion toward politics.
 1428

1429 To determine how far $\mathbf{e}_{b,u}^{(t_i)}$ travels along the chosen direction, the **magnitude of movement** is regu-
 1430 lated as:
 1431

$$mag^{(t_i)} = \text{Softplus}\left(\mathbf{W}_m \cdot \mathbf{W}_h \cdot \mathbf{e}_{b,u}^{(t_{i-1})}\right), \quad (22)$$

1433 where $mag^{(t_i)}$ acts like the *distance* of the walk, dictating whether the model advances cautiously
 1434 or moves decisively.
 1435

$$\mathbf{e}_{\mathbf{c}_{b_{u_j}}}^{(t_i)} = \mathbf{e}_{b,u}^{(t_i)} + mag^{(t_i)} \left(\cos \theta^{(t_i)} \cdot u^{(t_{i-1})} + \sin \theta^{(t_i)} o^{(t_i)} \right). \quad (23)$$

1438 This ensures that preference evolution is represented as a directed step, combining alignment with
 1439 historical momentum and deviation toward orthogonal novelty. For Alice, this means her reading
 1440 trajectory can smoothly extend within climate science when $\theta^{(t_i)}$ is small and $mag^{(t_i)}$ is low (steady
 1441 interest), or make a decisive turn into politics when $\theta^{(t_i)}$ is large and $mag^{(t_i)}$ accelerates the shift
 1442 (sharp interest change).
 1443

1444 **G.2 WALK2PERS-ENCODER AS AN INSTANTIATION OF SWH**
 1445

1446 We now formalize how the Walk2Pers-encoder concretely realizes the SWH update (Eq. 3). For
 1447 reference, recall the SWH rule:
 1448

$$\begin{aligned} e_{b,u}^{(t+1)} &= e_{b,u}^{(t)} + \underbrace{\text{mag}(a^{(t)}) \left(\cos \theta(a^{(t)}) u^{(t)} + \sin \theta(a^{(t)}) o^{(t)} \right)}_{\Phi: \text{geometric step}} \\ &+ \underbrace{\Psi(h_t^+, h_t^-)}_{\text{dual memory}} + \underbrace{\delta \cdot \mathbf{1}[a^{(t)} = \text{summGen}]}_{\text{drift}}. \end{aligned} \quad (3)$$

1454 **Theorem G.1** (Walk2Pers instantiation of SWH). *With the definitions of Sec. 3.3.1, the*
 1455 *Walk2Pers-encoder update is exactly of the form Eq. 3.*
 1456

1457 *Detailed Sketch.* We match each component of Eq. 3 to the Walk2Pers.

1458 (A) **Geometric step.** The encoder produces two scalar heads $(\hat{m}_t, \hat{\theta}_t)$ for each action $a^{(t)}$:

$$1460 \quad \text{mag}(a^{(t)}) = \text{softplus}(\hat{m}_t) \geq 0, \\ 1461 \quad \theta(a^{(t)}) = \pi \cdot \sigma(\hat{\theta}_t) \in (0, \pi).$$

1463 These control the *length* and *orientation* of the step. Next, Walk2Pers maintains two orthogonal
 1464 unit axes: - $u^{(t)}$: the “momentum” direction, aligned with recent preference drift. - $o^{(t)}$: an orthogonal
 1465 “novelty” axis obtained via Gram–Schmidt. Together, these yield the geometric increment

$$1466 \quad \Phi_t = \text{mag}(a^{(t)}) (\cos \theta(a^{(t)}) u^{(t)} + \sin \theta(a^{(t)}) o^{(t)}).$$

1468 *Intuition:* This term says each action either pushes the state forward in a continuity-preserving
 1469 direction (small θ) or rotates into a novel axis (large θ), with strength controlled by $\text{mag}(a^{(t)})$.

1470 (B) **Dual memory.** Walk2Pers keeps two asymmetric accumulators:

$$1472 \quad h_t^+ = h_{t-1}^+ + m^{(t)} \odot c^{(t)}, \\ 1473 \quad h_t^- = h_{t-1}^- \odot (1 - m^{(t)}) + c^{(t)}.$$

1475 Here $m^{(t)} = \text{SoftMax}(W_h h^{(t-1)} + W_c c^{(t)})$ is an action gate, and $c^{(t)}$ is the content embedding.
 1476 Thus: - h^+ *reinforces* positively gated interactions (e.g. clicks), accumulating them additively. - h^-
 1477 *suppresses* negatively gated interactions (e.g. skips), attenuating old signals via $(1 - m^{(t)})$.
 1478

1479 The two lanes are blended with a learnable weight $\omega \in (0, 1)$:

$$1480 \quad h^{(t)} = \omega h_t^+ + (1 - \omega) h_t^-.$$

1482 Finally, a linear projection produces the memory contribution:

$$1483 \quad \Psi(h_t^+, h_t^-) = W_\Psi[h_t^+; h_t^-].$$

1485 *Intuition:* Unlike MDH, which forgets everything beyond the last step, this mechanism lets
 1486 Walk2Pers reinforce long-term positive signals while still allowing suppression of repeated dis-
 1487 interest. Thus Ψ injects non-Markovian, history-dependent bias into the walk.

1488 (C) **Drift.** For the `summGen` action, Walk2Pers triggers an extra *summary drift* term. A drift
 1489 vector $\delta = W_\delta \phi_\delta(x_t)$ is generated and added only when $a^{(t)} = \text{summGen}$:

$$1491 \quad \Delta^{(t)} = \delta \cdot \mathbf{1}[a^{(t)} = \text{summGen}].$$

1493 *Intuition:* This nudges the preference state toward more “condensed” representations when the user
 1494 explicitly asks for a summary, acknowledging that summarization requests are qualitatively different
 1495 from passive clicks or skips.

1496 Putting together (A)–(C), the Walk2Pers update rule is

$$1498 \quad e_{b,u}^{(t+1)} = e_{b,u}^{(t)} + \Phi_t + \Psi(h_t^+, h_t^-) + \Delta^{(t)},$$

1499 which is identical to Eq. 3. Hence Walk2Pers a concrete instantiation of the Structured Walk
 1500 Hypothesis. \square
 1501

1502 **Remark** By parameter restriction: setting $\Psi \equiv 0$ and $\delta \equiv 0$ collapses Walk2Pers to a pure
 1503 geometric update. Further restrictions recover PRW, ARW, and RWR as shown in Cor. D.2.

1505 G.3 WALK2PERS-DECODER DETAILS

1507 **Latent Summary Contextualization** The query b-node embedding $\mathbf{e}_{b_q,u}^{(t_{l+1})}$ predicted by the en-
 1508 coder represents a geometrical alignment infused entanglement of behavior duplet $\langle \text{genSumm}, s_q \rangle$.
 1509 The s_q represents the latent s-node embedding of the query document d_q . Since $\mathbf{e}_{b_q,u}^{(t_{l+1})}$ has in-
 1510 fused the learned action embedding, it becomes difficult for a decoder to feed on it and generate a
 1511 personalized summary. To address this, we extract the latent s-node embedding from $\mathbf{e}_{b_q,u}^{(t_{l+1})}$.

1512 **Latent s-Node Contextualizer.** Although latent s-node embedding $\hat{\mathbf{e}}_{s_q,u}^{(t_{l+1})}$ represents the user’s
 1513 personalized summary intention, it lacks the contextualization of the query document d_q . The base
 1514 **decoder** contextualizes d_q with $\hat{\mathbf{e}}_{s_q,u}^{(t_{l+1})}$ using cross-attention, and feeds to a summarizer decoder.
 1515 The query document \mathbf{e}_{d_q} serves as the query, and $\hat{\mathbf{e}}_{s_q,u}^{(t_{l+1})}$ acts as both key and value, resulting sum-
 1516 mary contextualized query embedding as:
 1517

$$\mathbf{e}_{d_q}^c = \text{SoftMax} \left(\frac{(\mathbf{W}_q \cdot \mathbf{e}_{d_q})^\top (\mathbf{W}_k \cdot \hat{\mathbf{e}}_{s_q,u}^{(t_{l+1})})}{\sqrt{d}} \right) \cdot (\mathbf{W}_v \cdot \hat{\mathbf{e}}_{s_q,u}^{(t_{l+1})}) \quad (24)$$

1521 This contextualizes the document to be summarized with the latent summary intention of the user,
 1522 but the query document \mathbf{e}_{d_q} lacks explicit user-preference representation.
 1523

1524 **User-based d-Node Encoding.** To incorporate explicit user preferences into the document repre-
 1525 sentation, we enrich the query document embedding with the user’s interaction history. Specifically,
 1526 the encoder of the summarizer model produces the base document embedding \mathbf{e}_{d_q} . In parallel, the fi-
 1527 nal user history vector $\mathbf{e}_{b_q,u}^{(t_l)}$ from the `Walk2Pers` encoder is applied as a gating signal to modulate
 1528 \mathbf{e}_{d_q} , yielding the user-aware document embedding:
 1529

$$\mathbf{e}_{d_q,u} = \sigma(\mathbf{W}_g \cdot \mathbf{e}_{b_q,u}^{(t_l)}) \odot \mathbf{e}_{d_q}, \quad (25)$$

1532 The gating makes the query document align with the user’s own preference, while irrelevant aspects
 1533 are suppressed. This ensures the document is passed through the lens of Alice for generating the
 1534 expected summary for her, and the same document passes through the lens of Bob for generating his
 1535 expected summary. $\mathbf{e}_{d_q,u}$ encodes both the semantic content of the document and the personalized
 1536 preference profile of the user, enabling more faithful contextualization in subsequent cross-attention.
 1537 The latent s-node then contextualizes $\mathbf{e}_{d_q,u}$ to produce $\mathbf{e}_{d_q,u}^c$, as discussed in Section 3.3.2.
 1538

1539 **Personalized Summarization.** The `Walk2Pers` decoder generates a personalized summary by
 1540 feeding on contextualized query document embedding $\mathbf{e}_{d_q,u}^c$. We use the T5-base (Raffel et al.,
 1541 2020) decoder for the summarization.
 1542

1543 **Decoder Training.** The decoder training objective (\mathcal{L}_{dec}) is a linear combination of two loss func-
 1544 tions, *Generation Loss* (\mathcal{L}_{gen}) and the earlier encoder loss (\mathcal{L}_{enc} ; see Section 3.3.2), as $\mathcal{L}_{\text{dec}} =$
 1545 $\beta \cdot \mathcal{L}_{\text{gen}} + (1 - \beta) \cdot \mathcal{L}_{\text{enc}}$. Here, \mathcal{L}_{gen} is the cross-entropy loss between predicted tokens \hat{y} and
 1546 ground-truth y^* under teacher forcing with the T5 decoder. Optimizing \mathcal{L}_{gen} updates the cross-
 1547 attention layers and language-modeling head of T5 decoder, contextualizer weights \mathbf{W}_k , \mathbf{W}_q , \mathbf{W}_v
 1548 and inverse-mapping weights $\mathbf{W}_{\text{summ}}^+$, \mathbf{W}_c^+ . Fine-tuning the cross-attention layers ensures that the
 1549 decoder learns how to properly fuse the contextualized document embedding $\mathbf{e}_c^{(d_q,u_j)}$ with the
 1550 latent s-node embedding, thereby injecting user-specific preference signals into the decoding process,
 1551 and fine-tuning the language modeling head adapts the token generation distribution to reflect this
 1552 personalized conditioning, improving lexical and stylistic alignment with the user’s history. This
 1553 ensures accurate latent s-node reconstruction $\hat{\mathbf{e}}_{s_q,u}^{(t_{l+1})}$ and stronger cross-attention with document
 1554 embedding, thus improving summary relevance.

1555 All notations related to methodology are enumerated in Table 11.
 1556

1557 H IMPLEMENTATION DETAILS

1559 H.1 COMPUTE RESOURCES

1561 All data preprocessing (behavior graph generation, embedding lookup, and probability space map-
 1562 ping) was performed on CPU machines with 16GB memory per core. Embedding tables for news
 1563 bodies, headlines, and summaries were initialized using a shared vector space seeded from pre-
 1564 trained transformer T5-base encoder model Raffel et al. (2020). All training and inference experi-
 1565 ments for `Walk2Pers` were conducted using mixed-precision (FP32) training on L40S and A100
 1566 GPUs. We gratefully acknowledge Lightning.ai for providing virtual compute resources with A100
 1567

1566 and L40S GPUs. `Walk2Pers` utilizes almost 95% cheaper resource utilization and costs than the
 1567 best baseline LLM DeepSeek-R1. We summarize the detailed training and deployment details of
 1568 `Walk2Pers` in comparison to best LLM DeepSeek-R1 inference in Table 12.
 1569

1570 H.2 TRAINING 1571

1572 Model training was conducted end-to-end across the full pipeline for 6 epochs (approx. 20 hours),
 1573 and then with frozen encoder for 18 epochs (approx. 35 hours), over 63K unique behavior se-
 1574 quences. Optimization employed Adam (PyTorch v2.0.1) with learning rate of 1×10^{-3} . The
 1575 decoder operated with teacher-forced supervision using T5, with a learned adapter vector injected
 1576 as the decoder token in the first layer to guide personalized generation. Loss was a weighted
 1577 combination of classification loss over encoding of nodes, behavior node prediction and cross-entropy
 1578 loss on the personalized summary output. Hyperparameter details are in Table 13.
 1579

1580 H.3 T5 MODEL 1581

1582 The Text-to-Text Transfer Transformer (T5) (Raffel et al., 2020) is a unified framework that casts
 1583 all NLP tasks, ranging from translation and summarization to question answering and classification,
 1584 into a text-to-text format. This design choice enables the use of a single model architecture and
 1585 training objective across a diverse set of tasks. The T5 model is built upon the standard Transformer
 1586 architecture and is trained on a large corpus called the “Colossal Clean Crawled Corpus” (C4).
 1587 Among its variants, T5-base consists of 12 Transformer layers in both the encoder and decoder,
 1588 with a hidden size of 768 and 16 attention heads, totaling approximately 770 million parameters.
 1589

1590 **Decoder.** The decoder in T5 follows the autoregressive language modeling paradigm, predicting
 1591 the next token conditioned on previous outputs and the encoder’s representations. It incorporates
 1592 a stack of masked self-attention layers, encoder-decoder cross-attention layers, and feed-forward
 1593 layers. Unlike the encoder, which allows full bidirectional attention, the decoder’s self-attention is
 1594 causal (i.e., left-to-right masked) to prevent information leakage during training and inference. Each
 1595 decoder layer attends to both the previously generated tokens and the encoder outputs, enabling
 1596 the model to align and condition generation on the input sequence effectively. Position-wise feed-
 1597 forward layers and layer normalization are used after each attention block. During fine-tuning, the
 1598 decoder is trained to generate task-specific outputs, such as summaries or translations, making it
 1599 central to the T5’s generalization across tasks.
 1600

1601 I DETAILED RESULTS 1602

1603 I.1 HUMAN-JUDGMENT INTERPOLATION FROM OPENAI-REDDIT DATASET. 1604

1605 The interpolation of human judgment scores is performed by leveraging the OpenAI-Reddit dataset,
 1606 which provides multiple human-rated summaries for each article. For every article, the highest-
 1607 rated human summaries (7 out of 7) are designated as the *benchmark reference*. All candidate
 1608 summaries, including the benchmark, are first embedded into a high-dimensional semantic space
 1609 using a SentenceTransformer (Reimers & Gurevych, 2019) model. The semantic deviation between
 1610 the benchmark embedding V_b and any other summary embedding V_o is quantified via the Root Mean
 1611 Square Deviation (RMSD), which in this context is equivalent to the Euclidean distance:
 1612

$$1613 \text{RMSD}(V_b, V_o) = \sqrt{\sum_{i=1}^n (b_i - o_i)^2}.$$

1614 In practice, this computation is implemented efficiently using NumPy’s linear algebra module,
 1615 `np.linalg.norm`. The resulting RMSD values are then grouped according to the original hu-
 1616 man rating of each summary (e.g., 7/7, 6/7). By averaging the RMSD values within each rating
 1617 group, we obtain a mapping between human-judged quality scores and embedding-space distances.
 1618 Notably, the RMSD for summaries rated 7/7 is not always zero, as there may exist multiple distinct
 1619 summaries with a top score for the same article; while all such summaries are judged as equally
 high-quality by humans, their semantic embeddings can still differ due to variations in phrasing,

1620 emphasis, or lexical choices. These aggregated averages form the scoring thresholds used for inter-
 1621 polating human judgment in our evaluation framework.
 1622

1623 **I.2 ABLATION ON CLICK-ONLY TRAJECTORIES.**

1624 We ablate `Walk2Pers` under click-only trajectories, which results in highly imbalanced action dis-
 1625 tributions to investigate whether dual-memory components degenerate when skip actions become
 1626 extremely sparse. We observe that removing the geometric aligner leads to a moderate degra-
 1627 dation (avg. -0.08), reaffirming that sparsity weakens cross-action disentanglement. However, the
 1628 dual-memory encoder still remains stable and continues to extract preference signals from docu-
 1629 ment transitions, outperforming all competing baselines even in this extreme regime. Although
 1630 `Qwen-3` shows the smallest range of degeneration of performance w.r.t. the original performance,
 1631 `Walk2Pers` consistently outperform and show moderate degeneration. These results confirm that
 1632 (i) the geometric aligner is necessary for full robustness under skewed action distributions, and (ii)
 1633 the dual-memory lanes themselves do not collapse, even when skip/summarize actions nearly dis-
 1634 appear. Results are in Table 15.
 1635

1636 **I.3 ABLATION ON LOW FREQUENCY TOPICS.**

1637 We also ablate on 200 subset trajectories from the test data to understand whether rare, infrequent
 1638 but relevant topics get oversuppressed by the memory lanes or geometric novelty of `Walk2Pers`.
 1639 These 200 trajectories have a higher topic frequency (121 vs. 105) and a higher rate of topic change
 1640 within a trajectory (0.63 vs. 0.54) than the entire test dataset, indicating the occurrence of rare, infre-
 1641 quent topics within these trajectories. We find that although there is a degradation in performance,
 1642 the model still extracts stable user preferences, validating that the design principle of incorporating
 1643 learnable memory lanes and a geometric novelty aligner is necessary to understand users' evolving
 1644 interests in any real-world setting. Detailed results are in Table 16.
 1645

1646 **I.4 CROSS-TASK PERFORMANCE**

1647 As a further validation of `Walk2Pers` encoder, we evaluate the sequential recommendation perfor-
 1648 mance of it on widely adopted MIND news recommendation dataset. We find `Walk2Pers` encoder
 1649 (Full, with geometric step), which was trained end-to-end for personalized summarization task, to
 1650 surpass the MIND recommendation leaderboard baselines by a significant margin. It outperforms
 1651 the best baseline (Fastformer+PLM-NR-Ensemble) by $1.2\uparrow$ on MRR, $1.8\uparrow$ on nDCG@5, and $3.5\uparrow$
 1652 on nDCG@10. This result demonstrates the cross-task transferability of `Walk2Pers` encoder. De-
 1653 tailed results are in 17.
 1654

1655 **I.5 PERFORMANCE W.R.T. ACCURACY.**

1656 We evaluate the accuracy of `Walk2Pers` w.r.t. gold-reference summaries under standard accuracy
 1657 evaluation metrics Rouge-L and Rouge-SU4 (Lin, 2004), and find that `Walk2Pers` outperforms
 1658 the baselines by an average margin of $22.3/24.1$ on RG-L and RG-SU4, respectively. This confirms
 1659 that a boost in personalization capability also bridges the lack of accuracy gap. Results are in Table
 1660 18.
 1661

1662 **J PROMPT SETUP**

1663 **2-shot w/ history.** This setup provides the model with a complete user history that includes inter-
 1664 actions with previous articles in the form of clicks, skips, and summaries. Two in-context examples
 1665 are shown before the actual task, where each example contains the article content and a personaliza-
 1666 tion headline rewritten by the user. These few-shot examples serve as demonstrations to help the model
 1667 learn the structure of the desired output. Given a new query document, the model is instructed to
 1668 generate a personalized headline by considering the user's history: `click` indicates positive inter-
 1669 est, `skip` indicates disinterest, and `summarized` indicates focused preference. The headline is to
 1670 be returned in a specified format.
 1671

1674

1675

1676

1677

1678

1679

1680

1681

1682

1683

1684

1685

1686

1687

1688

1689

1690

1691

1692

1693

1694

1695

1696

1697

1698

1699

1700

1701

1702

1703

1704

1705

1706

1707

1708

1709

1710

1711

1712

1713

1714

1715

1716

1717

1718

1719

1720

1721

1722

1723

1724

1725

1726

1727

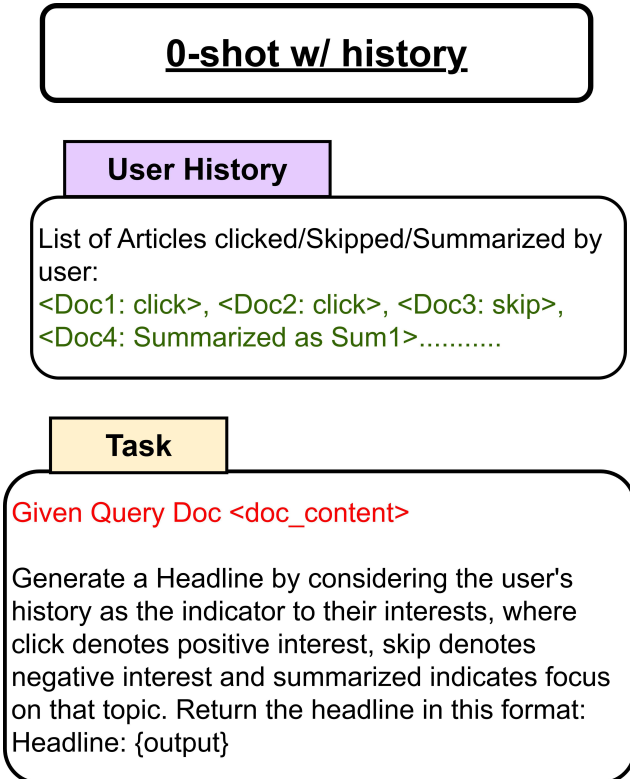


Figure 5: 0-shot Prompt-Template for LLM baselines.

0-shot w/ history. In this variant, the user history is again presented as a list of past interactions including clicks, skips, and summarizations, but no in-context examples are shown. Instead, a single task prompt is provided that explains the significance of each action type. The model is instructed to directly use this user history to infer the user’s interest and produce a personalized headline for a given query document. This prompt relies on the model’s zero-shot reasoning capabilities without relying on demonstrations.

Prompt-Chaining w/ history. This method adopts a multi-stage interaction design. In the first step, the model receives a single document and a user action (e.g., click), and is asked to extract topics, keyphrases, and user preferences based on that interaction. The output of each step is accumulated to incrementally build a structured user profile. As new interactions (e.g., skips or summaries) occur, the model is repeatedly prompted to refine or update the user’s inferred preferences. Finally, when the query document is given, the model uses the constructed user preference profile to generate a personalized headline. This setup simulates long-term personalization via chaining and stateful interaction across multiple prompts.

1728

1729

1730

1731

1732

1733

1734

1735

1736

1737

1738

1739

1740

1741

1742

1743

1744

1745

1746

1747

1748

1749

1750

1751

1752

1753

1754

1755

1756

1757

1758

1759

1760

1761

1762

1763

1764

1765

1766

1767

1768

1769

1770

1771

1772

1773

1774

1775

1776

1777

1778

1779

1780

1781

2-shot w/ history

User History

List of Articles clicked/Skipped/Summarized by user:

<Doc1: click>, <Doc2: click>, <Doc3: skip>,
<Doc4: Summarized as Sum1>.....

2 shot examples

[doc_content]
[Personalized Headline]: Rewritten_Titles by User

[Doc Content]
[Personalized Headline]: Rewritten_Titles by User

Task

Given Query Doc <doc_content>

Generate a Headline by considering the user's history as the indicator to their interests, where click denotes positive interest, skip denotes negative interest and summarized indicates focus on that topic. Return the headline in this format:
Headline: {output}

Figure 6: 2-shot Prompt-Template for LLM baselines.

Table 11: **Notations** used across Sections 3–4 and the Appendix. We group symbols by (i) the User–Interaction Graph (UIG), (ii) hypotheses and structured walk components (SWH), and (iii) the Walk2Pers instantiation (encoder, contextualizer, decoder).

Symbol	Explanation
User–Interaction Graph (UIG)	
$G = \langle N, E \rangle$	User–Interaction Graph with nodes N and edges E
$u^{(t_0)}$	User node at initial timestep t_0
$d^{(t)}$	Document node at timestep t
$s_j^{(t)}$	Summary node at timestep t for $d^{(t-1)}$
$a^{(t)}$	Action at time t (click, skip, genSumm, summGen)
$b_u^{(t)}$	Behavior duplet $(a^{(t)}, t l^{(t)})$ (action + tail node)
τ^u	User trajectory (ordered sequence over t)
$\mathcal{T}_{\text{train}}, \mathcal{T}_{\text{test}}$	Training and test trajectory pools
Hypotheses & Structured Walk (MDH vs. SWH)	
$e_{b,u}^{(t)}$	Latent preference state at b-node b after timestep t
$f(\cdot)$	One-step update under MDH (short-memory)
q	Recency prior (e.g., restart distribution in graph diffusion)
$\epsilon^{(t)}$	Stochastic perturbation in MDH updates
$\Sigma(a^{(t)})$	Action-conditioned covariance of $\epsilon^{(t)}$
$\Phi(\cdot)$	Geometric step: continuity vs. novelty (SWH)
$\Psi(\cdot)$	Dual memory: reinforcement (h^+) vs. suppression (h^-)
$\Delta(\cdot)$	Drift: special action-induced shift (e.g., summGen)
$u^{(t)}$	Momentum axis at t (continuity direction)
$o^{(t)}$	Orthogonal novelty axis at t
$\text{mag}(a^{(t)})$	Step magnitude (strength of update)
$\theta(a^{(t)})$	Step orientation angle (mix $u^{(t)}$ vs. $o^{(t)}$)
h^+, h^-	Positive/negative memory lanes (click reinforcement / skip suppression)
δ	Summary-specific drift vector (active for summGen)
Walk2Pers Encoder (b-layer), Sec. ??	
$f^{(a,t)}$	Action-gate function inside a b-cell at time t
$\mathbf{e}_{\text{tl}}^{(t)}$	Raw tail-node embedding at time t
$\mathbf{e}_a^{(t)}$	Action embedding (4-d one-hot or learned) at time t
$\mathbf{c}_{\text{tl}}^{(t)}$	Tail-cell content (flowing history) at time t
\mathbf{W}_{clk}	Click-specific projection used for cold-start at t_0
\mathbf{W}_b	Projection to b-node space
$\mathbf{e}_{b,u}^{(t)}$	b-node embedding produced by the b-cell at t
$\mathbf{h}^{(t)}$	Combined memory state at time t
$\mathbf{h}^{(+,t)}, \mathbf{h}^{(-,t)}$	Positive (reinforcement) / Negative (suppression) lanes
$m^{(t)}$	Gate for memory routing/strength (e.g., SoftMax over features)
$\Delta^{(t)}$	Drift vector injected on summGen, $(\mathbf{I} - \mathbf{e}_{\text{tl}}^{(t-1)}) \mathbf{e}_{\text{tl}}^{(t)}$
$\theta^{(t)}$	Predicted orientation angle at time t
$u^{(t-1)}, o^{(t)}$	Momentum axis (from $t-1$), novelty axis (at t)
$\text{mag}^{(t)}$	Predicted step magnitude at time t
$\mathbf{e}_{b,u}^{c(t)}$	Contextualized b-node after applying Φ, Ψ, Δ
\mathbf{W}_{next}	Linear head to predict next b-node embedding
$\mathbf{e}_{q,b,u}^{(t+1)}$	Predicted next b-node embedding (query b-node)
$W_{\text{pos}}^{(t)}$	Position classifier weight for alignment objective
$\hat{\mathbf{p}}_b^{(t)}$	Predicted position distribution for alignment
$\mathcal{L}_{\text{align}}, \mathcal{L}_{\text{next}}, \mathcal{L}_{\text{enc}}$	Encoder objectives: position alignment, next-b-node, joint
Latent Summary Contextualization (Decoder-side signals)	
$\hat{\mathbf{e}}_{s_q,u}^{(t_{l+1})}$	Latent s-node (summary-intent) for document d_q
\mathbf{e}_{d_q}	Base query-document embedding (backbone encoder)
$\mathbf{e}_{d_q,u}$	User-aware doc embedding (gated by trajectory state)
$\mathbf{e}_{d_q}^c$	Doc embedding contextualized by latent s-node
$\mathbf{e}_{d_q,u}^c$	Final user-conditioned doc embedding for decoding
W_q, W_k, W_v	Cross-attention projections (query, key, value)
W_g	Gating projection for $\mathbf{e}_{d_q,u}$
W_{summ}^+, W_c^+	Inverse-mapping weights used to extract latent s-node
Decoder Objective	
\mathcal{L}_{gen}	Token-level generation loss (cross-entropy, teacher forcing)
\mathcal{L}_{dec}	Decoder objective: $\beta \mathcal{L}_{\text{gen}} + (1 - \beta) \mathcal{L}_{\text{enc}}$

1836

1837 Table 12: Training and Deployment Resources Summary of **Walk2Pers** in comparison to best
1838 LLM baseline DeepSeek-R1.

Metric	Our Model (170M)	2-shot LLM (14B)	Relative Gain
Parameters	170M	14B	82 \times smaller
Avg. summary length	20 tokens	20 tokens	–
FLOPs/summary	2.04×10^{10}	1.68×10^{12}	82 \times lower
Inference time (per summary, est.)	0.2–2 s	15–160 s	60–80 \times faster
Running cost (GPU-hours)	18	42	orders lower
VRAM footprint	<1 GB	>28 GB	edge-deployable

1845

1846

1847 Table 13: Learned Weights and Hyperparameters of **Walk2Pers**.

Component	Shape / Type	Notes / Init
Training Configuration		
Batch size	38	Fixed across encoder/decoder
Optimizer	AdamW	PyTorch 2.0 impl.
Learning rate (end-to-end)	2×10^{-4}	End-to-end Training
Learning rate (decoder finetuning)	3×10^{-3}	Decoder fine-tuning
Epochs	6 + 18	6 joint, 18 decoder-only
Action Encodings		
$e_{\text{clk}}, e_{\text{skp}}, e_{\text{summ}}, e_{\text{sumgen}}$	4	One-hot action basis
$W_{\text{clk}}, W_{\text{skp}}, W_{\text{summ}}, W_{\text{sumgen}}$	(768, 4)	Action transforms, no bias
State & Memory Transforms		
W_{pull}	(768, 1)	Skip attraction transformation
W_s, W_d	(768, 768)	State transforms
W_h, W_c	(768, 768)	Memory routing gates
h^+, h^-	768	Reinforcement / suppression memories
$\omega^{(t)}$	scalar	Memory lane mixing weight; learnable
Fusion Layers		
W_h, W_c, W_z	(768, 768)	Fusion linear transforms
b_z	3	Fusion bias (zeros)
W_{emb}	(768, 768), bias 768	Embedding proj., std init
b_{emb}	768	Zeros init
Geometric Step (Orientation and Magnitude)		
W_{angle}	(768, 768)	Transforms to direction signal
W_{θ}	(1, 768)	Orientation angle transformation
W_h	(768, 768)	Shared with fusion
W_m	(1, 768)	Magnitude scaling transformation
$\theta^{(t)}$	scalar	Orientation angle, $(-\pi, \pi)$
$mag^{(t)}$	scalar	Step magnitude
Prediction / Decoder		
W_b	(768, 768)	Tail \rightarrow b-node proj.
$W_{\text{next}}, b_{\text{next}}$	(768, 768), 768	Next-node prediction
W_{pos}	(768, 768)	Positional alignment classifier
W_q, W_k, W_v	(768, 768)	Cross-attention projections
W_g	(768, 768)	User-aware doc gating
W_{summ}^+, W_c^+	(768, 768)	Inverse mapping for latent s-node
Complexity		
Per-step	$O(d)$	For each b-cell update
Condensed b-layer	$O(pd), p \ll T$	Long-horizon compression
Decoder	$\sim O(Ld^2)$	Transformer (T5-base)

1878

1879

1880 Table 14: **RQ-1/2: Next b-node Prediction (PENS Dataset) – Mean (μ) & Standard Deviation
1881 (σ):** Standard Deviation of SOTA MDH user-encoders is close to the Mean, thereby strengthening
1882 the reported performance gain; \dagger NT: Originally published results were on the *news recommendation*
1883 task in contrast to next behavior prediction.

Metric	NAML \dagger	NRMS \dagger	EBNR \dagger	Walk2Pers-Enc. w/o Geo. (mean)	Walk2Pers-Enc. Full (mean)
MRR$_{\mu}$	0.001	0.0009	0.0009	<i>0.121</i>	0.23
MRR$_{\sigma}$	0.0163	0.008	0.0101		
nDCG@5$_{\mu}$	0.0004	0.0002	0.0003	<i>0.082</i>	0.198
nDCG@5$_{\sigma}$	0.0176	0.01	0.012		
nDCG@5$_{\mu}$	0.0007	0.0004	0.0005	<i>0.132</i>	0.249
nDCG@5$_{\sigma}$	0.0199	0.0128	0.0146		

1890
 1891
 1892 Table 15: Performance degradation under sparse-click evaluation. Left value indicates the original
 1893 score; right value indicates sparse-click score; percentage drop from original values under this sub-
 1894 set. Lower drop indicates better robustness to interaction sparsity.
 1895

Model (Sparse Click-only Test)	PSE-JSD	PSE-SU4	PSE-METEOR
DeepSeek-R1-14B (2-shot)	0.248/0.147 (-40.7%)	0.094/0.064 (-31.9%)	0.097/0.071 (-26.8%)
Gemini-2.5-Flash (2-shot)	0.222/0.122 (-45.0%)	0.104/0.061 (-41.3%)	0.124/0.070 (-43.5%)
Qwen3-235B-Thinking (2-shot)	0.105/0.103 (-1.9%)	0.082/0.073 (-11.0%)	0.082/0.071 (-13.4%)
Best MDH Baseline (GTP)	0.024/0.016 (-33.3%)	0.170/0.009 (-94.7%)	0.019/0.011 (-42.1%)
Walk2Pers (w/o Geometric Step; Only Dual Memory)	0.306/0.231 (-24.5%)	0.334/0.253 (-24.3%)	0.321/0.234 (-27.1%)
Walk2Pers (Full)	0.452/0.378 (-16.4%)	0.383/0.301 (-21.4%)	0.449/0.310 (-31.0%)

1900
 1901
 1902
 1903
 1904
 1905 Table 16: Performance on Top 200 Low–Topic–Frequency Trajectories. Left value indicates the
 1906 original score; right value indicates sparse-click score; percentage drop from original values under
 1907 this subset. Lower drop indicates better robustness to topical sparsity.
 1908

Category	Model	PSE-JSD	PSE-SU4	PSE-METEOR
Best Baseline Variants	DeepSeek-R1-14B	0.248/0.091 (-63.3%)	0.094/0.074 (-21.3%)	0.097/0.082 (-15.5%)
	Gemini-2.5-Flash	0.222/0.092 (-58.6%)	0.104/0.081 (-22.1%)	0.124/0.083 (-33.1%)
	Qwen-3-235B-Thinking	0.105/0.094 (-10.5%)	0.082/0.073 (-11.0%)	0.082/0.077 (-6.1%)
	GTP (Best MDH)	0.024/0.016 (-33.3%)	0.170/0.013 (-92.4%)	0.019/0.015 (-21.1%)
Walk2Pers Variants	Walk2Pers (w/o Geometric Step)	0.306/0.280 (-8.5%)	0.334/0.290 (-13.2%)	0.321/0.280 (-12.8%)
	Walk2Pers-Full	0.452/0.410 (-9.3%)	0.383/0.320 (-16.4%)	0.449/0.380 (-15.4%)

1913
 1914
 1915
 1916
 1917 Table 17: RQ-3(b): Sequential Recommendation on MIND-Large. (sorted by MRR) Baselines show
 1918 paper-reported means. Walk2Pers results are reported with mean \pm variation from resampling.
 1919

Methods (Venue, Year)	AUC	MRR	nDCG@5	nDCG@10
DKN (WWW'18)	64.07	30.42	32.92	38.66
GRU (Baseline, 2016)	65.42	31.24	33.76	39.47
EBNR (KDD'17)	65.46	31.26	32.18	39.04
NPA (KDD'19)	65.92	32.07	34.72	40.37
NAML (IJCAI'19)	66.46	32.75	35.66	41.40
LSTUR (ACL'19)	67.08	32.86	35.95	40.94
Linear Transformers (ICML'20)	67.76	32.94	35.91	41.97
ProFairRec (SIGIR'22)	67.64	33.08	35.32	41.67
NRCLS (Appl. Sci.'24)	68.35	33.12	36.70	43.03
Linformer (arXiv'20)	68.02	33.19	36.22	42.10
Poolingformer (ICML'21)	68.54	33.20	36.69	42.60
NRMS (EMNLP-IJCNLP'19)	67.66	33.25	36.28	41.98
BigBird (NeurIPS'20)	68.14	33.28	36.42	42.18
Transformer (NeurIPS'17)	68.22	33.32	36.35	42.23
GERL (WWW'20)	68.10	33.41	36.34	42.03
GNewsRec (IP&M'20)	68.15	33.45	36.43	42.10
FIM (ACL'20)	67.87	33.46	36.53	42.21
HieRec (ACL-IJCNLP'21)	68.33	33.86	36.83	42.65
DCAN (arXiv'22)	68.90	33.90	36.90	42.80
ANRS (arXiv'22)	69.20	34.10	37.10	43.00
TCCM (CIKM'23)	69.75	34.42	37.53	43.25
Fastformer (arXiv'21)	69.11	34.55	37.62	43.38
FUM (SIGIR'22)	69.90	34.60	37.70	43.40
CAUM (SIGIR'22)	70.04	34.71	37.89	43.57
DIGAT (Findings ACL'22)	70.08	35.20	38.46	44.15
PLM-NR (SIGIR'21)	70.64	35.39	38.71	44.38
Fastformer+PLM-NR (Hybrid)	71.04	35.91	39.16	45.03
MINER (Findings ACL'22)	71.51	36.06	39.56	45.21
CAST-Rec (TOIS'25)	<u>72.10</u>	36.90	40.20	46.30
Fastformer+PLM-NR-Ensemble (Hybrid'22)	72.68	<u>37.45</u>	<u>41.51</u>	46.84
Walk2Pers-Full Encoder	53.32 \pm 1.1	38.64 \pm 1.8	43.32 \pm 1.2	50.38 \pm 1.4

1944

1945

1946 Table 18: Comparison of Specialized and Vanilla Models with `Walk2Pers` under standard accuracy metrics ROUGE-L/SU4
1947

Category	Model	Rouge-SU4	Rouge-L
	PENS-NAML-T1	13.12	21.62
	PENS-EBNR-T1	12.16	20.73
	PENS-EBNR-T2	12.41	20.82
Specialized (Personalized)	PENS-NRMS-T1	13.15	20.75
	PENS-NRMS-T2	13.64	21.03
	GTP-TrRMIo	21.91	28.31
	SP-Individual	19.54	25.18
	LLaMA-13B	18.31	29.54
LLMs w/ 2-shot history)	Mistral-7B	16.42	22.85
	DeepSeek-14B	19.57	29.72
	Zephyr-7B	18.45	26.45
Walk2Pers	Walk2Pers-Full	43.09	47.16

1957

1958

1959

1960

1961

Prompt-Chaining w/ history

1962

1963

1964

User History

1965

List of Articles clicked/Skipped/Summarized by user one by one:
 <Doc1: click>

1966

1967

1968

Task

1969

Given doc and action performed <doc1_content, click>

1970

1971

1972

Generate a list of interested keyphrases, topics, and preferences for the user.

1973

1974

1975

1976

Output

1977

1978

1979

1980

1981

Interest: <topic1, topic2, topic3>
 Keyphrases: <phrase1, phrase2, phrase3>

1982

1983

1984

1985

1986

1987

User History

1988

1989

1990

1991

1992

1993

1994

1995

1996

1997

List of Articles clicked/Skipped/Summarized by user one by one:
 <Doc2: skip>

Task

Given doc and action performed <doc1_content, click>, and the user preference output

Update a list of interested keyphrases, topics, and preferences for the user.

Figure 7: Prompt-Chaining Template for LLM baselines.